



**NIST Special Publication 260
NIST SP 260-266**

**Stability Testing for Standard
Reference Material[®] 2492 (Bingham
Paste Mixture): Testing procedure
clarification and improvements**

Kenneth Snyder

Gavin Donley

This publication is available free of charge from:

<https://doi.org/10.6028/NIST.260.266>



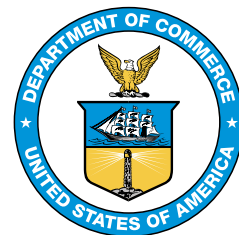
**NIST Special Publication 260
NIST SP 260-266**

**Stability Testing for Standard
Reference Material[®] 2492 (Bingham
Paste Mixture): Testing procedure
clarification and improvements**

Kenneth Snyder
Gavin Donley
Engineering Laboratory

This publication is available free of charge from:
<https://doi.org/10.6028/NIST.260.266>

April 2026



U.S. Department of Commerce
Howard Lutnick, Secretary

National Institute of Standards and Technology
Craig Burkhardt, Acting Under Secretary of Commerce for Standards and Technology and Acting NIST Director

Certain equipment, instruments, software, or materials, commercial or non-commercial, are identified in this paper in order to specify the experimental procedure adequately. Such identification does not imply recommendation or endorsement of any product or service by NIST, nor does it imply that the materials or equipment identified are necessarily the best available for the purpose.

NIST Technical Series Policies

[Copyright, Use, and Licensing Statements](#)

[NIST Technical Series Publication Identifier Syntax](#)

Publication History

Approved by the NIST Editorial Review Board on 2026-03-27

How to cite this NIST Technical Series Publication:

K.A. Snyder and G.J. Donley (2026) Stability Testing for Standard Reference Material[®] 2492 (Bingham Paste Mixture): Testing procedure clarification and improvements . (National Institute of Standards and Technology, Gaithersburg, MD), NIST Special Publication (SP) NIST SP 260-266.

<https://doi.org/10.6028/NIST.260.266>

Author ORCID iD

K.A. Snyder: 0000-0002-6015-9991

G.J. Donley: 0000-0002-5174-5024

Contact Information

kenneth.snyder@nist.gov

NIST SP 260-266

April 2026

Abstract

Periodic stability testing is conducted on a Standard Reference Material (SRM) to determine whether the current measured value is consistent with the SRM Certificate value. Stability testing performed on SRM 2492 (Bingham Paste Mixture), and the identical paste portion of SRM 2493 (Bingham Mortar Mixture), indicated evidence that some of the corn syrup specimens used in SRM 2492 may have changed; there was no evidence of similar changes in the corn syrup used for SRM 2493. As a result of this stability testing, sales of SRM 2492 have ceased. Fortunately, the paste portion of SRM 2493 is identical to SRM 2492 in both composition and proportion, and can be used as a direct replacement of SRM 2492. In addition, measurement procedures documented during the creation of the SRMs were reviewed and clarified, and in some cases processes were improved upon. The net effect of the improvements was to reduce the measured dynamic viscosity relative expanded uncertainty in the mean by at least a factor of 3, and as much as a factor of 7 across a considerable range of shear rates.

Keywords

cementitious; construction; paste; preshear; rheology; Standard Reference Material; viscosity.

Table of Contents

Executive Summary	1
1 Introduction	3
2 Materials and Equipment	7
2.1 SRM Components	7
2.1.1 Corn Syrup	7
2.1.2 Distilled Water	7
2.1.3 Limestone Powder	7
2.2 SRM Proportioning	9
2.3 Roughness Calibration Oil	10
2.4 Rheometer	10
2.4.1 Temperature Control	10
2.4.2 Evaporation Control	11
2.5 Planetary Centrifugal Mixer	12
3 Preparatory Methods	13
3.1 Sealing Jars	13
3.1.1 Corn Syrup Mixing Procedure	13
3.1.2 Paste Mixing Procedure	14
3.2 Syrup-Water Mixture Viscosity	14
3.3 Roughened Fixtures	15
3.3.1 Preparing Machined Fixtures	16
3.3.2 Establishing Zero Gap	17
3.3.3 Rotational Rheometry Notation	19
3.3.4 Fixture Roughness Calibration Regression	19
3.3.5 Fixture Roughness Viscosity Measurement	21
3.4 Selecting the Measurement Gap	21
4 Measurement Methods	24
4.1 SRM Measurement Methods	24
4.1.1 Rheometer Preparation	24
4.1.2 Sample Loading	25
4.1.3 SRM Procedure	26
4.2 SRM Procedure Path Dependence	27
4.3 Paste Preshear	28

4.3.1	Paste Preshear Method	29
4.3.2	Preshear Stress Relaxation	29
4.3.3	Preshear Efficacy	30
5	Results	33
5.1	Data Analysis	33
5.1.1	Viscosity vs. Shear Rate	33
5.1.2	Expanded Uncertainty in the Mean	34
5.1.3	Bingham Parameter Estimation	35
5.2	Corn Syrup Solution Viscosity	39
5.3	SRM Procedure Results	39
5.3.1	Paste Viscosity	39
5.3.2	Bingham Parameters	42
5.4	Preshear Procedure Results	43
5.4.1	Paste Viscosity	43
5.4.2	Bingham Parameters	45
5.5	Combined Results: C4-L16, C2-L6, and C2-L8	45
5.6	Viscosity vs. Water Content	48
6	Conclusions and Recommendations	50
6.1	SRM 2492 (Paste)	50
6.2	SRM 2493 (Mortar)	51
6.3	SRM 2492 Substitution	51
6.4	Reduced Measurement Uncertainty	51
6.5	Paste SRM Next Steps	52
	References	54

List of Tables

Table 1.	SRM 2492, and the paste portion of SRM 2493, component masses and the corresponding mass proportions.	9
Table 2.	SRM 2492, and the paste portion of SRM 2493, mass proportions expressed in a way to facilitate adding limestone powder to the corn syrup and water mixture.	9
Table 3.	The dynamic viscosity, as a function of temperature, of the commercial reference oil used to calibrate the fixture roughness.	10
Table 4.	Planetary centrifugal mixer procedure for 50 g sample of water and corn syrup: revolutions per minute (RPM), and mixing duration.	14
Table 5.	Planetary centrifugal mixer procedure for 50 g sample of paste: revolutions per minute (RPM), and mixing duration.	15

Table 6.	SRM 2492 Certificate Bingham parameter values for yield stress and plastic viscosity, within the first 24 hours; uncertainties represent the expanded uncertainty.	35
Table 7.	The Herschel-Bulkley model parameters and standard uncertainties estimated from logarithmically spaced evaluations of a cubic spline through the Certificate values of viscosity vs. shear rate.	37
Table 8.	The yield stress and plastic viscosity (and standard uncertainties) estimated from linearly spaced shear rates from a regression to the Herschel-Bulkley model using the logarithmically spaced Certificate values.	37
Table 9.	Corn syrup solution viscosity for each of the four sample boxes: (Paste) C4-L16 and C5-L19; and (Mortar) C2-L6 and C2-L8. Each value in the top four rows is the average of 5 replicate measurements on the same specimen, but each row represents an independent replicate. Below the top four rows are the column average \bar{x} and sample standard deviation s_x	39
Table 10.	Bingham plastic viscosity and yield stress using the SRM Procedure. The column mean (\bar{x}) and sample standard deviation (s_x) are shown.	43
Table 11.	Bingham plastic viscosity and yield stress using the Preshear Procedure. The column mean (\bar{x}) and sample standard deviation (s_x) are shown.	45

List of Figures

Fig. 1.	Evidence of an insoluble residue on the limestone as a result of adding excess DI water to the limestone: (a) after using a vortex mixer and centrifuge; and (b) after removing the supernatant and repeating the vortex mixing a second time.	8
Fig. 2.	Commercial rheometer vapor trap comprising two half shells, sitting on circular spacers: (a) the trap is closed, as when performing measurements; and (b) the trap is opened to show the mechanism for blocking vapor. For scale, the roughened plates have a diameter of 40 mm.	11
Fig. 3.	Commercial rheometer manufacturer's machined roughened fixtures: (a) top and bottom fixtures; (b) close up view of machined roughened surface. The circular roughened surface has a diameter of 40 mm	16
Fig. 4.	Magnified views of burrs on machined cross hatch plates, as delivered by the manufacturer. Each truncated pyramid is approximately 0.5 mm wide at its base.	17

Fig. 5.	Time dependent apparent viscosity showing the combination of drift (dashed straight line) and temperature equilibrium (solid curve). The viscosity values used in the subsequent analysis are the values at the y-intercept, denoted by the filled red circles. The legend shows the corrected gap H (mm).	22
Fig. 6.	The apparent viscosity η_a versus the corrected gap H : (a) the raw data; and (b) the inverses, along with the linear regression result.	23
Fig. 7.	Wind screen fashioned from a lidded jar, with bottom removed and then cut in half longitudinally; the halves are approximately 10 cm tall. In use, the halves are pushed together.	25
Fig. 8.	The typical response of an ascending path (UP) followed immediately by a descending path (DOWN) of the SRM procedure, which is similar to a constant total elapsed time measurement. The indicated torque (T) is expressed as a function of the indicated shear rate ($R\omega/H$).	27
Fig. 9.	A demonstration of the zero residual elastic stress in SRM 2492 for shear rates ranging from (0.1 to 10) 1/s. The dashed line is the strain for the $\dot{\gamma}_R = 10$ 1/s data, and is indicative of the strain for the other shear rates.	30
Fig. 10.	An example of the stress relaxation response when using the preshear method. The values in the legend are the indicated shear rates (in units of 1/s). The values that are averaged to establish an estimate for the torque are the 30 points shown in red.	31
Fig. 11.	A demonstration of the path independence afforded by the preshear: ascending followed by descending (UP-DOWN); periodically skipping measurement points (SAWTOOTH).	32
Fig. 12.	The logarithmic partial derivative of the torque (T) versus the shear rate ($\dot{\gamma}_R$) for a C4/L16 specimen.	34
Fig. 13.	Comparison of the SRM 2492 shear stress (σ), as function of shear rate ($\dot{\gamma}_R$), calculated from the Certificate values (filled circles), a cubic spline through those data (dashed line), and the Certificate Bingham equation (straight line).	36
Fig. 14.	The Herschel-Bulkley and the Bingham regression of shear stress (σ) on shear rate ($\dot{\gamma}_R$) for the same specimen made from C4-L16: (a) and (b) SRM Procedure; (c) and (d) Preshear Procedure.	38
Fig. 15.	Flow curves for the SRM 2492 (Paste) specimens (C4/L16 & C5/L19) using the SRM Procedure: (a) all the measured data are shown, with the mean value shown as a dashed line; and (b) the expanded uncertainty in the mean, compared with the SRM expanded uncertainty.	41

Fig. 16.	Flow curves for the SRM 2493 (Mortar) paste-component specimens (C2/L6 & C2/L8) using the SRM Procedure: (a) all the measured data are shown, with the mean value shown as a dashed line; and (b) the expanded uncertainty in the mean, compared with the SRM expanded uncertainty.	41
Fig. 17.	Data from C5/L19: (a) individual data compared with those of C4/L16; and (b) the expanded uncertainty in the mean compared with Certificate values.	42
Fig. 18.	Flow curves for the SRM 2492 (Paste) specimens (C4/L16 & C5/L19) using the Preshear Procedure: (a) all the measured data are shown, with the mean value shown as a dashed line; and (b) the expanded uncertainty in the mean, compared with the SRM expanded uncertainty.	44
Fig. 19.	Flow curves for the SRM 2493 (Mortar) paste-component specimens (C2/L6 & C2/L8) using the Preshear Procedure: (a) all the measured data are shown, with the mean value shown as a dashed line; and (b) the expanded uncertainty in the mean, compared with the SRM expanded uncertainty.	44
Fig. 20.	SRM procedure flow curves for the C4/L16, C2/L6, and the C2/L8 boxes: (a) all the data, with the mean value shown as a dashed line; and (b) the expanded uncertainty in the mean (Triple), compared with the SRM expanded uncertainty (SRM).	46
Fig. 21.	Preshear procedure flow curves for the C4/L16, C2/L6, and the C2/L8 boxes: (a) all the data, with the mean value shown as a dashed line; and (b) the expanded uncertainty in the mean (Triple-PS), compared with the SRM expanded uncertainty (SRM).	46
Fig. 22.	Comparison of SRM Procedure vs. preshear results from samples C4-L16, C2-L6, and C2-L8. Mean and expanded uncertainty in the mean are shown.	47
Fig. 23.	Relative expanded uncertainty in the mean (U/\bar{x}) throughout the shear rate range for the combined data from the three specimens C4/L16, C2/L6, and C2/L8: SRM procedure; and preshear method. For comparison, the SRM Certificate relative expanded uncertainty is approximately 0.15 throughout the shear rate range.	48

NIST SP 260-266

April 2026

Author Contributions

K.A. Snyder: Conceptualization, Methodology, Analysis, Drafting and Writing.

G.J. Donley: Conceptualization, Methodology, and Writing.

Executive Summary

The National Institute of Standards and Technology (NIST) developed Standard Reference Material (SRM) 2492 (Bingham Paste Mixture for Rheological Measurements) to meet two objectives. The first objective was to create a viscosity SRM with Certificate values that were similar to those from fresh ordinary portland cement pastes. This was achieved through a mixture of corn syrup, water, and finely ground limestone powder. This SRM can be used to calibrate non-standard rheology testing geometries, and can be used to help standardize measurement methods for these types of pastes.

The second objective was to use this SRM as the matrix for SRM 2493 (Bingham Mortar Mixture for Rheological Measurements) and SRM 2497 (Bingham Concrete Mixture for Rheological Measurements), each of which combines SRM 2492 with spherical glass beads to represent the effects fine aggregate (SRM 2493) and both fine and coarse aggregate (SRM 2497). The primary purpose of SRM 2493 (Mortar) and SRM 2497 (Concrete) is to calibrate mortar and concrete rheometers, respectively. This is accomplished by using each SRM's certified values for its Bingham parameters (plastic viscosity and yield stress) and its dynamic viscosity as a function of shear rate.

This report is a summary of the steps taken to perform the periodic stability testing for SRM 2492 (Paste) and SRM 2493 (Mortar). The stability testing is conducted to ensure that the properties are consistent with the certified values. The stability testing for the two different SRMs was simplified by exploiting the fact that the addition of the glass spheres to the paste SRM changes the viscosity in a known way, meaning that only the paste portion of SRM 2493 (Mortar) was tested. Furthermore, the paste portion of SRM 2493 is identical to SRM 2492 in both composition and proportions; i.e., the values can be compared directly. Because the stability testing procedure required for SRM 2493 (Mortar) was identical to that for SRM 2492 (Paste), this report refers the the stability testing of both SRMs as the stability testing of SRM 2492.

The sample preparation and measurement procedures that were used to create SRM 2492 and SRM 2493 were documented in NIST publications. In the case of rheological measurements on pastes, these procedures must be adhered to exactly. During this stability testing, a number of the documented procedures were clarified or improved upon. The updated techniques spanned sample preparation, instrument setup, and material measurement: mixing and measuring the viscosity of the corn syrup solution; calibrating the fixture roughness and ensuring a consistent zero point; mixing the paste; and measuring the paste viscosity. The net result of these improvements was to reduce the relative expanded uncertainty in the mean (confidence: $1-\alpha = 0.95$) by at least a factor of 3, and as much as a factor of 7 across a considerable range of shear rates. These revised techniques are discussed in detail.

The SRM sampling consisted of obtaining two boxes of SRM 2492 and two boxes of SRM 2493 from the NIST SRM Program. The stability testing indicated that the corn syrup in both SRMs has changed. In general, the corn syrup solution viscosity has decreased from the value reported

during the SRM development, and the resulting SRM 2492 paste viscosity versus shear rate has changed. In addition, an isolated dramatic change was observed in one of the corn syrup specimens; three of the four SRM samples being tested were nearly identical to one another, but the fourth sample was significantly different.

For the three similar SRM samples, the magnitude of the change in paste viscosity is in proportion to the change in the corn syrup solution. It was observed that if the corn syrup solution viscosity is greater than 0.130 Pa·s, the expanded uncertainty in the viscosity vs. shear rate overlaps the expanded uncertainty of the Certificate values. Below this critical corn syrup solution viscosity, however, adherence to the Certificate values cannot be guaranteed.

The one SRM sample that was significantly different from the rest was from one of the SRM 2492 boxes, which has been in storage longer than SRM 2493. Given the occurrence of this outlier result, the possibility of other outliers in the current SRM 2492 stock cannot be ruled out. Therefore, it was decided to cease sales of SRM 2492, and to recommend using the paste portion of SRM 2493 as a direct substitution.

Using the paste portion of SRM 2493 as a replacement for SRM 2492 is not a viable permanent solution. SRM 2493 is more expensive than SRM 2492, which could suppress sales. Also, because the corn syrup used in SRM 2493 is identical in composition to SRM 2492, it is expected that it, too, will start to exhibit the same type of change that was observed for SRM 2492 during this stability testing.

In the future, an alternative to creating more SRM 2492 is to create a new NIST Research Grade Test Material (RGTM). Materials that could be used to develop stable and extensible RGTMs for paste rheology are discussed. Initially, these RGTMs might be used to develop consensus measurement techniques for different types of construction materials, and if demand for a specific reference material is great enough, NIST can develop a corresponding certified SRM.

1 Introduction

In the year 2000, an international comparison of commercial and research concrete rheometers [1, 2] was conducted by having each rheometer measure the same 12 concrete mixtures, and then report an estimated plastic viscosity and yield stress. Although the different rheometers reported values that varied by as much as an order of magnitude, the ranked order of the rheometer values was consistent across all the mixtures. The wide variation in the reported values was due to a number of factors: each rheometer used a different geometry, some rheometers were calibrated using a reference oil, and other rheometers merely calibrated the instrument torque. The industry recognized the need for a calibration reference material with properties similar to concrete, but viable commercial reference oils were expensive, and concrete rheometers require a large volume of fluid. It was concluded that an alternative, less expensive reference material was needed.

To meet this industry need, the National Institute of Standards and Technology (NIST) began a long-term research program to create a Standard Reference Material (SRM) for calibrating concrete rheometers. The material had to have rheological properties similar to concrete, and it had to be stable.

The work progressed in stages. First, an SRM was developed that replicated the rheological properties of an ordinary portland cement paste (i.e., portland cement powder and water). The resulting SRM is a mixture of an aqueous corn syrup solution and limestone powder. Next, 1 mm spherical glass beads were added to the paste SRM to approximate the rheological properties of a mortar. Finally, 1 cm spherical glass beads were added to the mortar SRM to approximate the rheological properties of a concrete. The resulting three rheology SRMs are as follows:

1. SRM 2492 (Bingham Paste Mixture for Rheological Measurements) [3, 4]
2. SRM 2493 (Bingham Mortar Mixture for Rheological Measurements) [5]
3. SRM 2497 (Bingham Concrete Mixture for Rheological Measurements) [6]

The accuracy of the mortar SRM and the concrete SRM is predicated on having an accurate estimate of the paste SRM viscosity. The paste SRM viscosity is measured experimentally, using parallel plate rotational rheometry. The mortar and concrete SRM viscosities are estimated, in part, from computer simulation; cup-and-bob rotational rheometry was used to validate the result for the mortar. For these simulations, the paste SRM flow curve (viscosity as a function of shear rate) is the critical input to a computational model that was used to estimate the relative change in viscosity that occurs due to the addition

of the glass beads. These relative changes are used to establish the SRM Certificate flow curve tables for the SRM 2493 (Mortar) and SRM 2497 (Concrete).

SRM 2492 (Paste) was developed to mimic the rheological properties of the fresh portland cement paste component of conventional concrete. The SRM is a mixture of three components (water, corn syrup, and fine limestone powder), which the customer combines and mixes prior to testing. The SRM 2492 Certificate [7] provides reference values for the dynamic viscosity as a function of shear rate (flow curve data), and for the Bingham plastic viscosity and yield stress, which are determined from a linear regression of the flow curve data: shear stress vs. shear rate. Once developed, SRM 2492 was then used as the foundation for developing SRM 2493 (Bingham Mortar Mixture for Rheological Measurements) [5] and SRM 2497 (Bingham Concrete Mixture for Rheological Measurements) [6] through the addition of spherical glass beads.

When an SRM is developed, it is assessed for the need to conduct periodic *stability testing* to determine whether the Certified values are still accurate; i.e., whether the certified material property has changed. At the time of SRM production, it was decided to perform periodic stability testing because it was conceivable that the corn syrup could change over time. This work is the result of stability testing for SRM 2492 (Paste) and SRM 2493 (Mortar). Because SRM 2493 differs from SRM 2492 in only the addition of 1 mm glass spheres, the stability testing of SRM 2493 consisted of testing its paste component, which is identical to SRM 2492 in both composition and proportions.

Using a parallel plate rotational rheometer to measure the viscosity of pastes, such as SRM 2492, presents a number of technical challenges. Because the system is viscoelastic, the time-dependent stress response of the system is a function of its time-dependent shear history [8]. This can include the shear rates of previous measurements, and the duration of each of these previous measurements [9]. Also, the viscosity is often inferred from the *steady-state stress at a constant shear rate*, but this, too, can be challenging. At very low shear rates there can be competing physical effects, preventing an unquestionable determination of *steady state*.

As a result, viscosity is often reported at a particular condition defined by the measurement process. The two most frequently used process definitions are to take each measurement either at a fixed elapsed time or at a fixed accumulated strain. But even then, the result can be measurement dependent. For example, in cases where shear thinning or thixotropy are significant [9], the measurement is only repeatable when one also specifies the number of measurements made per decade of shear rate.

Given this, the interpretation of SRM stability testing depends on the purpose of the SRM. If the purpose of the SRM is a set of reference data from which one can establish

repeatability for a given measurement method, one compares the Certificate values to the measured values, when performed in strict accordance of the original measurements.

By way of contrast, if the purpose of the SRM is to calibrate rheometers, the absolute accuracy of the estimated viscosity is vital because it is the primary means of standardizing the relationship between torque and shear rate for the complex geometries typically used in mortar and concrete rheometers. Given the technical challenges of uniquely determining the viscosity of a viscoelastic material, the more authoritative procedure would be to perform the measurement until there is evidence that the stress response has reached steady-state, as these are the only values with direct correspondence to rheometers with arbitrary geometry.

The Certificate values in SRM 2492 were established from constant time measurements [3, 4]. The measurement procedure was developed in the context of the rheology measurements of portland cement pastes. Because these cementitious systems hydrate, their properties are changing in time, so rheological measurements need to be performed quickly. In an effort to mimic measurement strategies for cement pastes, the SRM measurement procedure limited the total measurement time to 30 s at each shear rate, which is not enough time for the stress to equilibrate at the lower shear rates in the Certificate.

The stability testing was used as an opportunity to compare the measurement method specified for the Certificate to alternative measurement methods that are more representative of the equilibrium shear stress, at a given shear rate.

The stability testing consisted of measurements made from samples taken from the inventory of SRM 2492 (Paste) and SRM 2493 (Mortar); two specimens of each SRM. Measurements revealed that the viscosity of the corn syrup is changing. When water is added to the as-delivered corn syrup, the measured viscosity has decreased by amounts ranging from 8 % to 25 %. The effects of this change are borne out in the change in the paste viscosity flow curve. At the highest shear rates, the average measured values are within the expanded uncertainty of the Certificate values. At the lowest shear rates, however, the average measured values are outside the expanded uncertainty. Further investigation revealed that the inconsistency with Certificate values was due to one of the corn syrup specimens having changed considerably. A comparison among the three that were consistent among one another gave results within the expanded relative uncertainty of the SRM Certificate values.

Upon reviewing the measurement procedure referenced in the SRM Certificate, there were a few minor ambiguities. The stability testing was used as an opportunity to either clarify procedures or make changes that improved repeatability. These measurement improvements addressed the following:

Rheometer Fixture Roughness: Viscosity measurements of pastes require the instrument fixture to have a roughened surface to avoid slip between the specimen and the plate. The operator must determine the effective surface roughness for the purpose of correcting the shear rate (to account for the material moving “within” the roughened features). An updated procedure is given for which the reference oil viscosity is a fitting parameter. The accuracy of predicted oil viscosity is an indication of the quality of the calibration procedure.

Zero Gap: With roughened plates, the operator needs a means of establishing a consistent zero gap because as the plates rotate relative to one another (prior to establishing a zero), the “zero” can vary by over 100 μm . This was solved by lapping the fixture top surfaces, and using a gauge block during the gap zero-ing process.

Corn Syrup Solution Mixing: An alternative mixing approach, using a planetary centrifugal mixer, allows for smaller samples, and uses a mixing procedure that minimizes the amount of incorporated air.

Corn Syrup Solution Viscosity: At the time that the SRMs were developed, the viscosity of the corn syrup solution was measured using a vibratory insertion rheometer. An alternative method is proposed that uses the rotational rheometer. The accuracy of this method is critical for determining whether the corn syrup has changed.

Paste Viscosity Measurement: In addition to the measurement process provided in the original SRM report, a modified measurement method was also used. The modifications included measuring to constant total shear (at each shear rate), and using a preshear that made the measurements independent of the previous measurements. The constant shear requirement was needed to achieve constant shear stress, and the preshear was used to reduce the number of measurements required.

Bingham Model Parameters: The Bingham model parameters of yield stress and plastic viscosity are estimated from linear regression performed on stress vs. shear rate data. Because the data follow a curve (not a straight line), the range of shear rates and the number/location of shear rates influence the outcome of the regression. The SRM 2492 supplemental report indicates that the regression should be performed on uniform linearly spaced shear rate data, but viscosity flow curves (viscosity vs. shear rate) are typically performed on uniform logarithmically spaced shear rates. A method is proposed that fits the Herschel-Bulkley model to the logarithmically spaced data, from which the model is used to estimate values that are linearly spaced.

2 Materials and Equipment

The following describes the SRM component materials, as delivered for stability testing. This information applies to both SRM 2492 (Paste), and the paste component of SRM 2493 (Mortar). The information below is repeated from the SRM 2492 reports [3, 4] for convenience. The following also describes the equipment used that differed from the equipment used to initially develop SRM 2492.

Unless stated otherwise, all uncertainties express the standard error.

2.1 SRM Components

Although SRM 2492, as well as the paste component of SRM 2493, is a mixture of three components (water, corn syrup, and limestone powder), it is shipped with only the corn syrup and the limestone powder; the customer provides the distilled water.

2.1.1 Corn Syrup

At the time the SRM was created, the corn syrup was 100 % glucose (no additives), the water mass fraction was (0.186 ± 0.002) g/g, and the measured density was (1436 ± 5) kg/m³ [3].

2.1.2 Distilled Water

Distilled water was specified in the Certificate to ensure consistency. Testing laboratories lacking in-house water distillation can purchase distilled water at a local grocery or home improvement store. For these measurements, however, de-ionized water (nominally 18 M Ω -cm) was used.

2.1.3 Limestone Powder

The limestone powder is a commercial product, referred to as a micro-limestone flour, and advertised as passing a #325 sieve (45 μ m opening). Measurements performed at NIST include the density (2815 ± 5) kg/m³, and the Brunauer–Emmett–Teller (BET) surface area (1.05 ± 0.02) m²/g. The limestone mineral composition was approximately

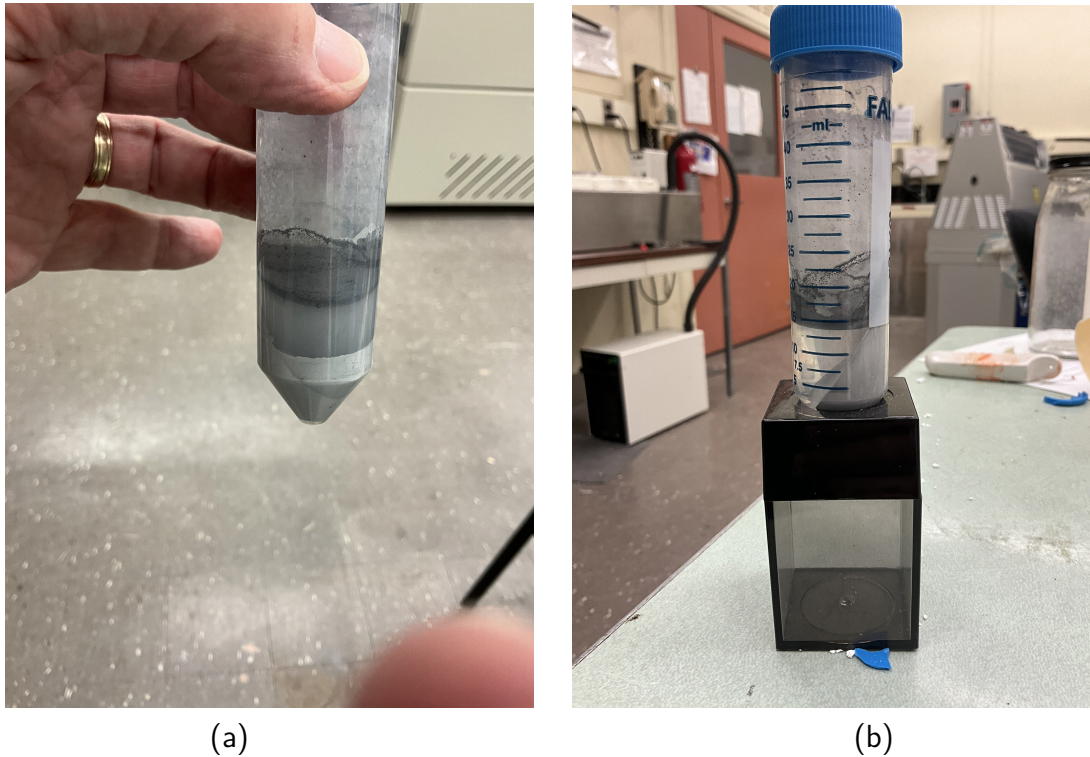


Figure 1: Evidence of an insoluble residue on the limestone as a result of adding excess DI water to the limestone: (a) after using a vortex mixer and centrifuge; and (b) after removing the supernatant and repeating the vortex mixing a second time.

75 % calcite, 20 % dolomite, and 2 % tremolite. Further details of the limestone analysis are in the 2012 report [3].

When the limestone is mixed with the corn syrup solution, black streaking might appear throughout the mixture. To determine the nature of this material, equal masses of de-ionized water and limestone powder were combined, mixed in a vortex mixer, and then centrifuged. Figure 1(a) shows a 20 g sample after a first iteration of mixing and centrifuging, and (b) shows the results after decanting the supernatant and repeating the process. The black material floats in water, suggesting it is insoluble residue, and would be consistent with a grinding aid used during the limestone powder production. Only after the fourth iteration was there no visible black material floating in the water.

This testing was performed to understand the origin of the black streaking. For the purpose of conducting the stability testing measurements, however, the limestone was used as delivered.

2.2 SRM Proportioning

The SRM 2492 report [3] provides the mass of each component for making a batch of the SRM, and the values are repeated in Table 1. The batch size is intended for creating specimens for mortar rheometers. To facilitate making smaller batches for testing with a parallel plate rheometer, the mass proportions are also given in Table 1.

Table 1: SRM 2492, and the paste portion of SRM 2493, component masses (from Ref. [3]) and the corresponding mass proportions.

Component	Certificate Mass (g)	Mass Proportion
Corn Syrup	200.0	1.0000
Distilled Water	63.16	0.3158
Limestone Powder	458.1	2.291

The corn syrup is the most difficult to portion out to an exact mass. Therefore, the corn syrup was portioned first, and the proportional amount of water was added. This is why the mass proportions in Table 1 are relative to the corn syrup mass.

Furthermore, the corn syrup solution (corn syrup and water) had to be mixed thoroughly before the addition of limestone powder. It was found to be easier to make a batch of corn syrup solution, portion out a sample, and add a precise amount of limestone powder. To facilitate this, the mass proportion of limestone powder, calculated from the original Certificate masses in Table 1 and relative to the corn syrup solution, is given in Table 2.

Table 2: SRM 2492, and the paste portion of SRM 2493, mass proportions expressed in a way to facilitate adding limestone powder to the corn syrup and water mixture.

Component	Mass Proportion
Water + Corn Syrup	1.0000
Limestone Powder	1.7408

To ensure accurate results, the samples were large enough to obtain sufficient significant digits in the mass measurements. The scale recorded to the nearest 0.1 mg, and each component mass was at least 1 g.

2.3 Roughness Calibration Oil

Parallel plate rotational rheometry measurements on paste specimens requires the use of roughened plates to ensure the material does not slip along the fixture surface. The region within the roughness contributes to the effective gap. To account for this, measurements are made with a reference fluid to estimate the effective width of the roughness.

Table 3: The dynamic viscosity, as a function of temperature, of the commercial reference oil used to calibrate the fixture roughness.

Temperature (°C)	Viscosity (Pa·s)
20.00	31.480
25.00	19.800
37.78	6.736
40.00	5.664
50.00	2.706

This roughness calibration testing used a commercial polybutene viscosity reference oil, which has the temperature dependence shown in Table 3. The measurements were conducted at 23 °C, so the assigned viscosity was estimated using regression. The logarithm of the viscosity values was regressed to a cubic function of the temperature. The maximum relative difference between the predicted viscosity and the values in Table 3 was 4.3×10^{-5} . Therefore, the estimated viscosity at 23 °C is (23.762 ± 0.001) Pa·s.

2.4 Rheometer

A strain-controlled rheometer was used to conduct the stability testing, which differs from the SRM development process, which used a stress-controlled rheometer. The strain-controlled rheometer has a *usable* torque range of 10 μ N.m to 20 mN.m. This range was adequate for measuring the viscosity of the corn syrup and water mixture, and the SRM pastes.

2.4.1 Temperature Control

The specimen temperature was controlled through a Peltier control system, which only controlled the temperature of the bottom plate; the upper fixture had a thermal heat

break to prevent thermal conduction from the laboratory air. Once the fixture reached equilibrium, the indicated temperature varied by less than 0.1 °C.

2.4.2 Evaporation Control

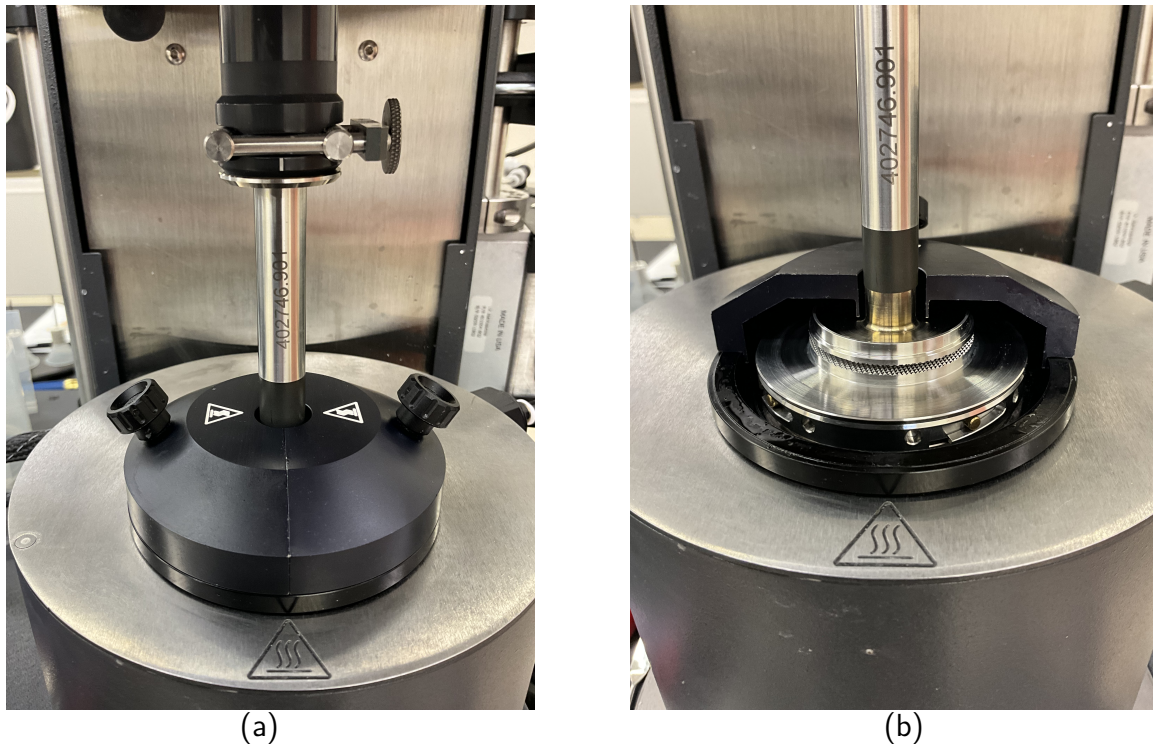


Figure 2: Commercial rheometer vapor trap comprising two half shells, sitting on circular spacers: (a) the trap is closed, as when performing measurements; and (b) the trap is opened to show the mechanism for blocking vapor. For scale, the roughened plates have a diameter of 40 mm.

During the original development of the SRM, moisture loss was minimized by surrounding the specimen with a sponge saturated with water. For these stability testing measurements, however, the rheometer manufacturer's vapor trap was used. The vapor trap relies on the top fixture having a shallow trough to hold water. The trap has two halves that envelope the fixture, and create a vapor barrier by having a "wall" that drops down into the trough; see Fig. 2 for details. This type of trap is common among commercial rheometers.

To improve the vapor trap effectiveness, the contact surfaces of the vapor trap components are coated with a thin film of mineral oil. Care is taken, however, to avoid getting mineral

oil into the top fixture water trough; a thin layer of oil on the surface of the water can reduce water vapor pressure in the chamber surrounding the specimen.

2.5 Planetary Centrifugal Mixer

The stability testing procedures relied on the use of a planetary centrifugal mixer, instead of the impeller mixer referred to in the SRM report [3]. The planetary mixer has the advantage of allowing for varying specimen volumes (from 10s of grams to 100s of grams), and minimizes the incorporation of air into the specimen.

3 Preparatory Methods

The following subsections describe techniques that either are not mentioned or are alternatives to the methods in the SRM reports [3, 4, 5].

3.1 Sealing Jars

SRM 2492 is a water-based paste. Therefore, the accuracy of a measurement will depend on the water content, and the property stability throughout a measurement procedure depends on the water content remaining constant over the course of a measurement.

To minimize the transport of moisture into or out of jars containing the corn syrup (i.e., via evaporation or adsorption), the as-delivered jar is lidded tightly and then sealed with a semi-transparent, flexible film comprising a blend of waxes and polyolefins. When sealing the jar, follow the film manufacturer's recommended practice to ensure a tight seal. When using other films, check to manufacturer's specifications to ensure that the jar contents do not alter the properties of the applied film.

Moreover, the film was used throughout the measurement process. The film was applied to the as-delivered jar of corn syrup, applied to lidded vials containing the water:corn syrup solution, and applied to lidded vials containing the small samples of paste.

3.1.1 Corn Syrup Mixing Procedure

The supplemental SRM 2492 report [3] instructs the operator to create 700 g batches at a time, and to mix the specimen using an insertion blender (akin to the ones used to mix milkshakes). The nature of an insertion blender means that the rate of shearing decreases rapidly with distance from the impeller. As a result, when mixing the water and corn syrup, it is difficult to ensure that all the corn syrup has been incorporated. Furthermore, the certificate mixing proportions require a relatively large quantity of material to be produced each time, for the implied use of creating a specimen for testing in a mortar or concrete rheometer. By contrast, a parallel plate rheometer specimen mass is on the order of 15 g, and the material is only certified for up to one week after mixing.

To facilitate smaller samples, an alternate mixing procedure was developed. A planetary centrifugal mixer was used to produce specimens that were less than 100 g. The corn syrup was added first, and then the water. The water and corn syrup were then mixed in

the planetary mixer using the protocol in Table 4. Prior to placing the specimen in the planetary mixer, the specimen jar is tilted and slowly rotated to help dislodge most of the sugar off the bottom of the jar, and to create a soft ball of sugar.

The slower initial planetary mixing speed is needed to help distribute the corn syrup and to avoid having the corn syrup become compacted in the center of the jar bottom. After the second (higher speed) stage there may be a very small amount of corn syrup attached to the jar bottom, and the final slower speed mixing will help to remove it.

Table 4: Planetary centrifugal mixer procedure for 50 g sample of water and corn syrup: revolutions per minute (RPM), and mixing duration.

RPM	Time (min)
1000.	3
2000.	3
1000.	1

Contrary to the recommended procedure in the SRM Certificate, the water:corn syrup mixture is made the day before, and left to rest. The next day, before testing or use, the specimen is given one more mix in the planetary centrifugal mixer at 1000. RPM¹ for 1 min. If left undisturbed for a period of time, the solution should be mixed again (e.g., 1000. RPM for 1 min).

3.1.2 Paste Mixing Procedure

The paste was also mixed using a planetary centrifugal mixer. The mixer imparts significant shear, while introducing relatively little air. The paste mixing times are shown in Table 5 below. Between each step, a metal spatula was used to ensure thorough mixing by scraping material away from the sides of the jar, and breaking up any large clumps of limestone. The objective is to mix sufficiently to eliminate observable black streaking.

3.2 Syrup-Water Mixture Viscosity

During the development of SRM 2492, the viscosity of the corn syrup and water mixture was evaluated with an insertion, vibratory viscometer, as noted in the SRM 2492 recertification report [4]. In that report, the corn syrup solution viscosity was estimated to be

¹1 RPM = $2\pi/60$ rad/s

Table 5: Planetary centrifugal mixer procedure for 50 g sample of paste: revolutions per minute (RPM), and mixing duration.

RPM	Time (s)
1000.	60
1000.	60
2000.	15

(0.159 ± 0.005) Pa·s at 23 °C. Assessing whether the corn syrup has changed requires an accurate measurement of the corn syrup solution viscosity.

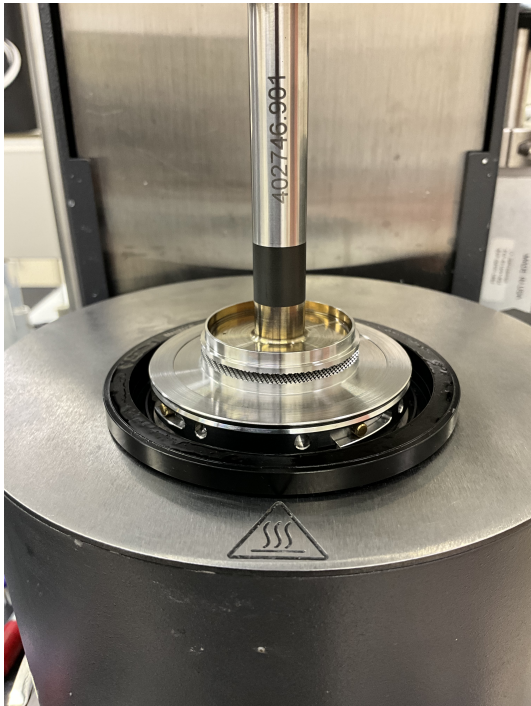
A recommended way of measuring the syrup-water mixture viscosity is to use the rheometer, equipped with either flat parallel plate or a cone and plate fixtures. To ensure consistency with the values from the recertification report, the rheometer should be held at 23 °C. The recommended measurement gap is 0.60 mm, and a number of shear rates should be tested to confirm Newtonian behavior. The minimum shear rate depends upon the minimum torque required to obtain consistent, accurate values, and the maximum shear rate is often dictated by the onset of material ejection.

3.3 Roughened Fixtures

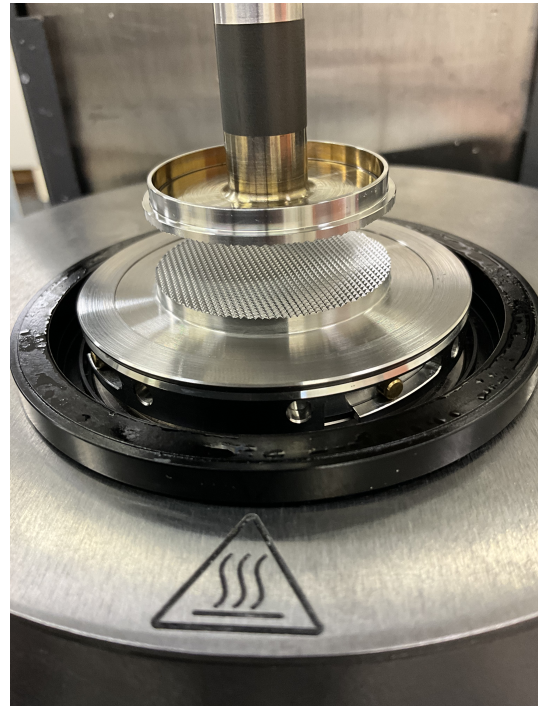
Rotational rheometry measurements on pastes require roughened fixture surfaces for the purpose of avoiding slip at the boundaries. As a general rule, the roughness features should have a length scale that is not less than the nominal largest size of particles in the paste.

A consequence of using roughened fixtures is that the true shear rate differs from the apparent shear rate. This arises because when fixtures are brought into contact, to establish a “zero” gap, the peaks of the roughness touch first. As a result, a method is needed for estimating a roughness parameter that relates the apparent shear rate (as calculated by the instrument) to the true shear rate (that accounts for the roughness).

The secondary challenge is establishing a consistent “zero” indicated gap. As the fixtures are rotated with respect to one another, the “zero” gap of the fixtures changes as the roughness “peaks” pass one another. This can also be true for the milled roughened surfaces on the fixtures sold by rheometer manufacturers.



(a)



(b)

Figure 3: Commercial rheometer manufacturer's machined roughened fixtures: (a) top and bottom fixtures; (b) close up view of machined roughened surface. The circular roughened surface has a diameter of 40 mm

3.3.1 Preparing Machined Fixtures

The roughened fixtures used for this stability testing were the *cross hatched* type sold by the rheometer manufacturer. The as-delivered machined roughened fixtures, however, required the following steps to ensure consistent roughness features across the entire surface of the fixture:

- Examine the surface, using a stereo microscope, for irregularities. These may include mis-shaped roughness features or deformities that leave behind large burrs because the intersection of the roughness features and the radius can result in very thin/small features that can be easily deformed.
- Deburr the roughened surface with a flexible pad made for that purpose (typically olive drab in appearance). See examples of the burrs found in the fixture surface in Fig. 4. The process should be done with great attention to detail, pausing periodically to review progress using a stereo microscope.

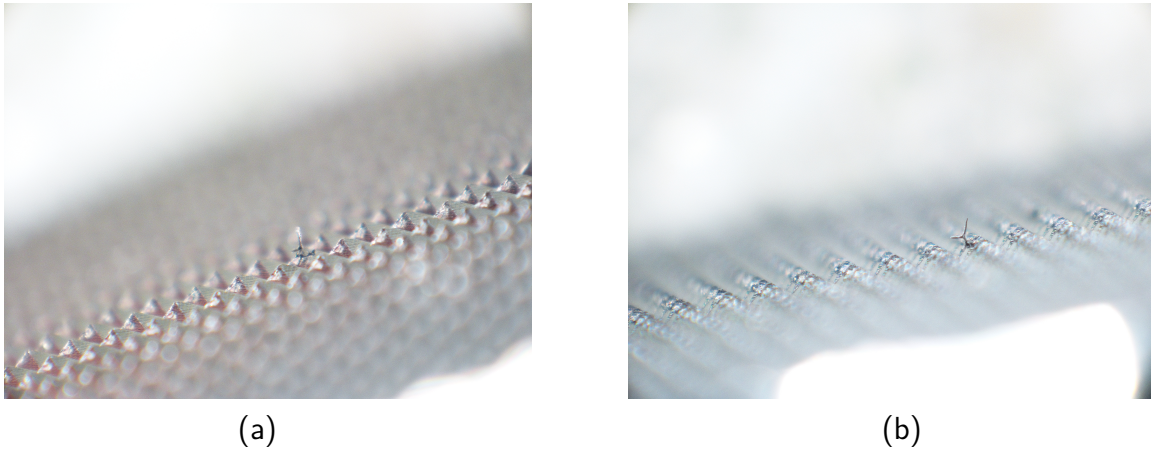


Figure 4: Magnified views of burrs on machined cross hatch plates, as delivered by the manufacturer. Each truncated pyramid is approximately 0.5 mm wide at its base.

- Flatten the top surface by lapping with 2000 grit sandpaper on a very flat surface; ex: using a float glass used for honing woodworking tools. This must be done with care to ensure that the two fixtures remain parallel to one another.

3.3.2 Establishing Zero Gap

Establishing a consistent zero gap ($H = 0$) is essential to obtaining repeatable measurement results. Generally, one uses the instrument to establish the point of zero gap. The instrument performs this by bringing the fixtures into contact, to a prescribed axial force, and reports that separation as the point of zero gap.

For roughened fixtures, however, that method of establishing zero gap can introduce considerable uncertainty to the overall measurement. If one records the axial force required to replicate an indicated zero gap, and then rotates the fixtures with respect to one another, the indicated gap (at the same axial force) might change by up to $100 \mu\text{m}$. For an intended gap of 0.6 mm, that variability represents a relative uncertainty of more than 15 %, and which means the final result cannot have a relative uncertainty less than this.

To remedy this, a method was developed to bring the plates to a consistent separation distance, which formed a consistent zero gap. This was done in two steps.

The first step is to determine the axial force corresponding to the indicated zero gap:

1. attach smooth/flat plate fixtures

2. use the rheometer to zero the gap
3. manually bring the plates back into contact (very carefully)
4. determine the axial force corresponding to an indicated zero gap

If the instrument allows the plates to rotate (with respect to one another during this process), using flat plates will give more consistent results. Although one could pick a zero offset axial force arbitrarily, using the “zero gap” axial force that the instrument uses would likely ensure consistency. Note, this step only needs to be performed once.

The second step requires a machinist’s gauge block to establish a consistent reference gap opening by performing the following steps:

1. attach roughened fixtures
2. use the instrument to zero the gap (standard testing procedure)
3. separate the fixtures
4. insert a machinist’s gauge block (e.g., 1 mm)
5. repeat the following steps
 - manually apply the axial force corresponding to zero gap
 - record the indicated gap spacing
 - open the gap and move/rotate either the gauge block or a fixture
6. calculate the average indicated gap with the gauge block

The differences among the indicated gaps with the gauge block inserted should be within a couple of micrometers of one another. If not, either the gauge block is unreliable, or the surfaces of the fixtures are no longer flat and parallel.

The gap is corrected for the difference between the gauge block thickness and the indicated gap with the gauge block inserted. For a gauge block of thickness Δ and an average indicated gap (with the gauge block inserted) δ , the corrected gap H of a future measurement performed at (instrument) indicated gap H° is calculated as follows:

$$H = H^\circ + \Delta - \delta \quad (1)$$

This gauge block correction must be applied each time the roughened surfaces are “zeroed.” This procedure is required for the SRM measurements, and for the roughness calibration discussed below.

3.3.3 Rotational Rheometry Notation

Rotational rheometry uses a short-hand notation for certain quantities because it is understood that the geometry confines the meaning of these quantities. For the analysis of SRM 2492, the rheological characterization focuses on the dynamic viscosity (η), which is the ratio of the shear stress to the shear rate. The shear stress (σ) is a tensor, but in ideal rotational rheometry (\hat{z} in vertical direction), only the $\sigma_{z\theta}$ component is relevant. Similarly, the shear rate is the rate-of-deformation tensor ($\dot{\gamma}$), but in ideal rotational rheometry, only the $\dot{\gamma}_{z\theta}$ component is relevant. As a result, in discussions of rotational rheometry, the tensor component subscripts are dropped: shear stress (σ), and shear rate ($\dot{\gamma}$).

For rotational rheometry using parallel smooth plates having constant gap H , the shear rate is a function of the radius r and the rotational frequency ω :

$$\dot{\gamma}(r) = \frac{r\omega}{H} \quad (2)$$

In many of the expressions relating the torque (T) to the viscosity, however, the calculations are often parameterized by the shear rate at the edge of the plate:

$$\dot{\gamma}_R = \frac{R\omega}{H} \quad (3)$$

For a Newtonian fluid, the dynamic viscosity (η) can be expressed as follows:

$$\eta(\dot{\gamma}_R) = \frac{2T}{\pi R^3 \dot{\gamma}_R} = \frac{\sigma}{\dot{\gamma}_R} \quad (4)$$

3.3.4 Fixture Roughness Calibration Regression

When using roughened parallel plates, the distance over which material is shearing is larger than the corrected gap H because the material “within” the roughness features contribute to the overall flow field. As a result, the roughness changes the interpretation of the gap between the plates, and the shear rate imposed on the specimen.

In practice, the true shear rate is less than the value reported by the instrument. This occurs because the instrument indicates a gap spacing H° of zero to be when the plates

touch. In reality, the true spacing is a combination of the indicated gap and some measure of the roughness ϵ .

During the development of the SRM, the roughness was estimated by finding the constant offset to the gap that resulted in a constant estimate for the fluid viscosity [10, 3, 4]. By contrast, the following is an alternative procedure that uses a functional relationship between the apparent and true viscosity to arrive at a linear relationship. The resulting regression parameters are a function of the roughness parameter and the true viscosity of the reference oil being used. The difference between the estimate reference oil viscosity and the reported reference oil viscosity serves as a measure of the quality of the measurement procedure.

Following the derivation by Connelly and Greener[11], the correction to the gap is made by assuming that the true gap can be expressed as the sum of the corrected gap H and a constant roughness parameter ϵ : $(H + \epsilon)$. The correction to the shear rate is derived using the method of Pipe et al. [12] and Kramer et al. [13]. Using a rotational rheometer to measure the viscosity of a reference oil, the steady-state shear stress σ can be expressed either as a function of the apparent shear rate $\dot{\gamma}_{Ra}(H)$ and apparent viscosity η_a (i.e., as would be reported by the instrument), or as a function of the true shear rate $\dot{\gamma}_{Rt}$ and the true viscosity η_t :

$$\begin{aligned}\sigma = \dot{\gamma}_{Ra} \eta_a &= \dot{\gamma}_{Rt} \eta_t \\ \frac{R\omega}{H} \eta_a &= \frac{R\omega}{H+\epsilon} \eta_t\end{aligned}\tag{5}$$

Solving for the apparent viscosity, one arrives at the following linear equation:

$$\eta_a^{-1} = (\epsilon \eta_t^{-1}) H^{-1} + \eta_t^{-1}\tag{6}$$

The coefficients are determined from a linear regression of the inverse apparent viscosity η_a^{-1} against the inverse corrected gap H^{-1} . The degree to which the true viscosity η_t , calculated from the fitting parameters, agrees with the reported viscosity of the fluid used in the measurement, is a measure of the quality of the overall measurement procedure.

The data for the regression are collected using the commercial viscosity reference oil described in Section 2.3, and by starting at a large gap and then making subsequent measurements at progressively smaller gaps (without reloading the specimen). The uncertainty in the roughness ϵ is estimated by propagating the uncertainties in the slope and intercept of Eqn. 6. Once the roughness parameter is calculated for a particular roughened surface, it is assumed that it is the appropriate correction for any specimen.

3.3.5 Fixture Roughness Viscosity Measurement

Even when using a commercial reference oil for calibrating the roughness factor, the measurement can be challenging. Although the reference oil has stable properties, reopening the measurement chamber (to trim the specimen) with each change in gap requires time for the temperature to equilibrate. In addition, even when testing in a vapor trap that has been sealed with mineral oil, the viscosity can change very slowly with time, due to some combination of factors.

It is assumed that the changes in the measured viscosity are due to the combined effects of temperature equilibration and drift. The former is characterized by an exponential function, and the latter is characterized by a linear function of time. At each gap, the 9 consecutive viscosity measurements (each 160 s in duration) are regressed to the following equation:

$$\eta_a(t) = at + b + ce^{-t/d} \quad (7)$$

In Eq. 7, the time t is the elapsed measurement time from the start of the 9 replicate viscosity measurements.

The data and regression results are shown in Fig. 5, for gaps ranging from 0.9 mm down to 0.3 mm. The function in Eq. 7 is shown as a solid line, and the linear portion is shown as a dashed line. The apparent viscosity η_a used for the gap is the linear intercept b from Eq. 7. In Fig. 5, this value is indicated by the red filled circle.

The resulting apparent viscosity η_a values are plotted in Fig. 6(a) as a function of the corrected gap H . The inverse values are plotted in Fig. 6(b), along with the regression result from Eq. 6.

The results of the regression shown in Fig. 6(b) are as follows:

$$\epsilon = (0.303 \pm 0.002) \text{ mm} \quad (8)$$

$$\eta_t = (23.82 \pm 0.10) \text{ Pa} \cdot \text{s} \quad (9)$$

At the measurement temperature of 23 °C, the reference oil viscosity was estimated to be approximately 23.76 Pa·s. Given that the regression estimate was within its standard error of the reference value, the quality of the overall measurement procedure is deemed good.

3.4 Selecting the Measurement Gap

The SRM 2492 (Paste) has sufficient water content that at high shear rates the material can be ejected (i.e., thrown) from between the plates. The propensity for this to happen

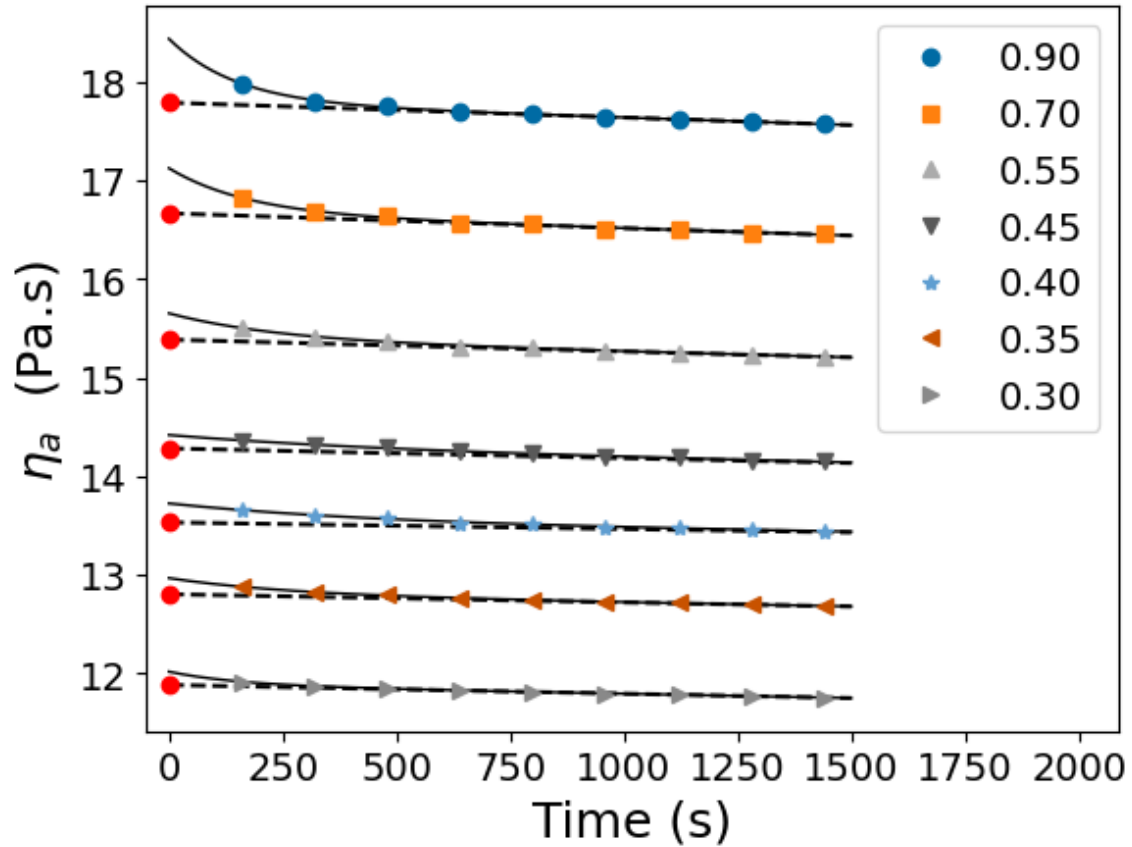


Figure 5: Time dependent apparent viscosity showing the combination of drift (dashed straight line) and temperature equilibrium (solid curve). The viscosity values used in the subsequent analysis are the values at the y-intercept, denoted by the filled red circles. The legend shows the corrected gap H (mm).

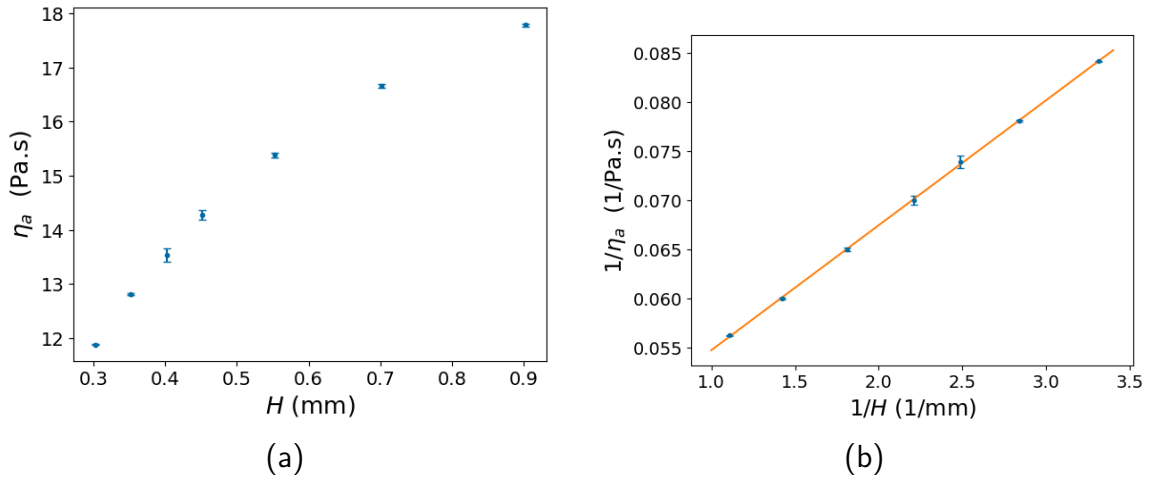


Figure 6: The apparent viscosity η_a versus the corrected gap H : (a) the raw data; and (b) the inverses, along with the linear regression result from Eq. 6 .

is a function of both the gap and the shear rate. The measurement effect of ejection is to reduce the observed viscosity because there is less material between the fixtures. Therefore, when there is evidence of ejection, smaller gaps must be used if the maximum shear rate cannot be changed.

The smallest allowable gap is dictated by the size of the largest particles in the paste. Generally, the indicated gap should be approximately 10 times the size of the largest particles in the paste. For SRM 2492, the largest particles are approximately $90 \mu\text{m}$. Given that the fixture roughness is on the order of $300 \mu\text{m}$, the smallest recommended indicated gap is on the order of 0.600 mm .

As the gap decreases below this limit, the particles can jam at high shear rates (there is less time for them to move around one another), and one observes anomalously greater viscosity.

4 Measurement Methods

4.1 SRM Measurement Methods

The measurements were conducted on a strain controlled rheometer, using standard parallel plate rotational rheometry techniques. The following provides additional information, for the purpose of ensuring that the procedure can be replicated.

Rotational rheometry can be challenging because the measurement results can depend on each step of the sample preparation and measurement. The staff who originally developed the SRMs are no longer at NIST, which precipitated the review of each step in detail. In some cases, the specifics are vague; they are either missing, or can be interpreted in a couple ways, or the details are spread across multiple reports. In addition, some of the procedures had to be adapted to the task of stability testing of small specimens.

4.1.1 Rheometer Preparation

The use of a vapor trap typically means that some portion of the top fixture is exposed to laboratory room air flow. Some manufacturers try to reduce the effect of room temperature by putting a “heat break” in the fixture post; a short section of low thermal conductivity. Depending on the measurement sensitivity, the results can still exhibit the effects of changing laboratory air temperature.

To help reduce the effects of changing laboratory room temperature, a make-shift shield was created from a large plastic jar. The jar bottom was cut off and the remainder was cut in half, longitudinally. The two halves surround the vapor trap, and the halves extend up so as to reduce room air flow across the fixture shaft; see Fig. 7 for clarification.

Even with the accessories to reduce the effect of temperature fluctuations, the instrument needs time to come to equilibrium at the measurement temperature. To do this, the following steps are taken:

- Set the temperature control to 23.0 °C
- Install the top and bottom fixture
- Assemble the vapor trap, with water
- Close the vapor trap

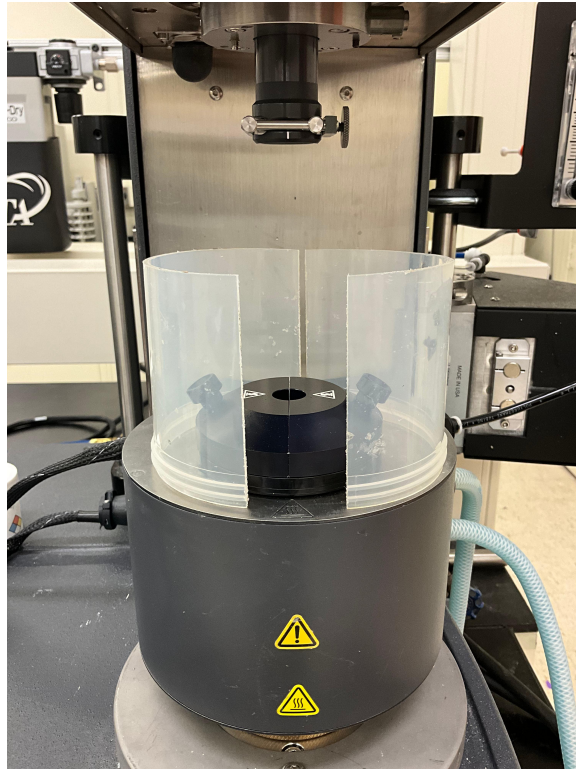


Figure 7: Wind screen fashioned from a lidded jar, with bottom removed and then cut in half longitudinally; the halves are approximately 10 cm tall. In use, the halves are pushed together.

- Use an additional enclosure, like that shown in Fig. 7, to minimize the effect of lab room air flow
- Let setup equilibrate to the measurement temperature

4.1.2 Sample Loading

When the instrument has come to equilibrium with the measurement temperature, the following specimen loading procedure is used for the corn syrup solution and the SRM paste:

- Remove the plastic jar wind break
- Open the vapor trap and move the fixtures to the loading gap

- Scoop (with a measuring spoon) material out of the sample jar and pour the material onto the bottom fixture
- Close the fixtures to the trim gap (measurement gap multiplied by 1.025)
- Trim excess material
- Close down to the measurement gap
- Close the vapor trap
- Replace the wind break

4.1.3 SRM Procedure

The following measurement procedure is replicated from the SRM reports. The data collection for the creation of the SRM included a correction for fixture roughness. Therefore, to report corrected shear rates up to the Certificate maximum of 35 1/s, the *indicated* shear rate has to be greater than this value. The corrected measurement gap is approximately 0.600 mm, and the roughness is approximately 0.300 mm, so the measurements should include a maximum shear rate of approximately 45 1/s.

When using the SRM flow curve testing method, the number of measurement points in the ascending and descending paths affect the outcome of the results [9]. For the purpose of reproducibility, the density of measurements is typically described by the number of shear rates that are uniformly spaced on a logarithmic scale, and referred to as *points per decade*.

The following is the measurement protocol used in the stability testing - the maximum *indicated* shear rate should be adjusted, as necessary, for the specific fixture roughness being used:

- Precondition: constant shear rate of 0.01 (1/s) for 150 s
- Flow curve *indicated* shear rate range (0.1 to 45) (1/s) - *spaced logarithmically*
- Ascending measurements (0.1 to 45) (1/s) - 7 points per decade
- Descending measurements (45 to 0.1) (1/s) - 9 points per decade

- At Each Point: terminate measurement step when there is less than 0.5 % change, but apply steady shear for no longer that 30 s.
- Analyze the data from the descending measurements

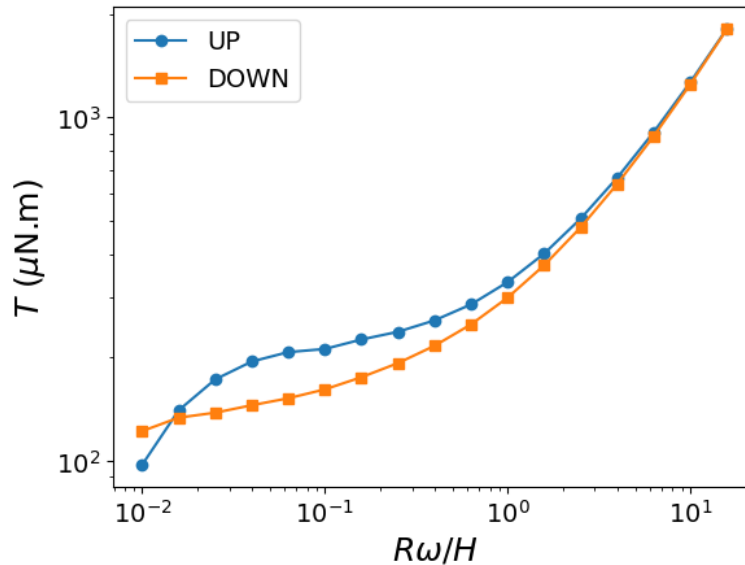


Figure 8: The typical response of an ascending path (UP) followed immediately by a descending path (DOWN) of the SRM procedure, which is similar to a constant total elapsed time measurement. The indicated torque (T) is expressed as a function of the indicated shear rate ($R\omega/H$).

4.2 SRM Procedure Path Dependence

The results from fixed elapsed time viscosity measurements depend strongly on the specific measurement path taken. The SRM 2492 measurement technique, consisting of an ascending path, followed by a descending path, is shown in Fig. 8; the measured torque T is plotted against the apparent shear rate $R\omega/H$. At the highest shear rates, there is sufficient time for the torque to reach equilibrium. At the lowest shear rates, however, each measurement along the ascending torque path does not reach equilibrium before moving on to the next measurement, so the subsequent measurements are still “experiencing” the higher viscosity of the previous measurement. By contrast, the corresponding measurements along the descending path begin each measurement with a material exhibiting a lower viscosity. For pastes like SRM 2492, the torque measured along ascending path is almost always greater than that of the descending path.

The results shown in Fig. 8 are typical for pastes, and the effects of measurement procedure on the results for a variety of pastes were studied in detail by Divoux [9]. Not only are the results of constant time measurements a function of the path, they can also depend on the duration of each measurement, and how many measurements are taken per decade of shear rate. For reproducibility, it is common for researchers to specify the conditions under which the measurements were taken. Therefore, to replicate the Certificate results, the prescribed measurement procedure must be adhered to precisely.

4.3 Paste Preshear

There are a number of limitations to the constant time measurement procedure used to develop the SRM. Most notably, the results depend on the number of measurement points per decade of shear rate. Interestingly, as the number of points per decade increases, the flow curves start to converge [9]. Unfortunately, this becomes an impracticality for pastes subject to sedimentation because of the measurement duration at very low shear rates.

For a reference material used to calibrate a rheometer, however, one would like a more absolute estimate of the viscosity. More specifically, a determination of the viscosity via a measurement method that does not depend on the path, nor on the number of measurements taken per decade of shear rate.

Conceptually, a preshear is a specific shearing procedure, applied before each measurement, that puts the material in a consistent microstructural *state*. The shear stress response from this state will be the same, regardless of all prior measurements. Also, combining a preshear with a constant total strain measurement provides a consistent assessment of equilibrium shear stress.

A distinct advantage of such an approach is that if the paste under study has properties consistent with an existing model (e.g., Herschel-Bulkley), there is a minimum number of measurements needed to estimate the model parameters to sufficient accuracy. Although constant total strain measurements (at the same points-per-decade) take longer than constant total time, if the number of measurement points can be reduced considerably, and a preconditioning ascending path eliminated, the total measurement time can be reduced.

4.3.1 Paste Preshear Method

A preshear was developed by Choi and Rogers (CR) [14], for model yield stress fluids, for the purpose of “...guaranteeing unbiased material states” in stress-controlled rheometry. In short, it is a method that removes all “information” about the shear history, thus putting the system in the same starting condition before each measurement.

The CR preshear was developed for stress-controlled rheometry and comprises three steps:

1. Constant rotation to achieve equilibrium stress;
2. Forced recovery (reverse the direction) until at a point of zero stress (remove residual elasticity); and
3. Rest (remain motionless) as a rebuilding time for thixotropic materials.

The CR preshear was modified for strain-controlled rheometry by adding a period of flow cessation after the initial constant rotation [15]. This step was added to dissipate viscous stress, leaving only stress due to elastic properties.

In strain-controlled rheometry, the amount of forced (strain) recovery has to be estimated from the material properties to ensure that the residual stress is nearly zero after the forced (strain). Stress growth and flow cessation were repeated on SRM 2492 at shear rates ranging from (0.1 to 10) 1/s, and the results are shown in Figure 9. In the figure, the dashed line indicates the applied strain for the $\dot{\gamma}_R = 10$ 1/s data; the other strain curves are omitted for clarity. Moreover, upon the application of constant shear, the stress reaches an equilibrium after a total strain of approximately 20.

Serendipitously, upon flow cessation the residual elastic stress in SRM 2492 is zero over the range of shear rates tested. As a result, a forced recovery is not required, and the preshear protocol is the following:

- Constant shear rate $\dot{\gamma}_R = 10$ 1/s for 3 s.
- Flow cessation for 5 seconds

4.3.2 Preshear Stress Relaxation

The measured torque vs. total strain for one of the specimens is shown in Fig. 10. The legend gives the indicated shear rate (in units of 1/s), and the red circles indicate the 30

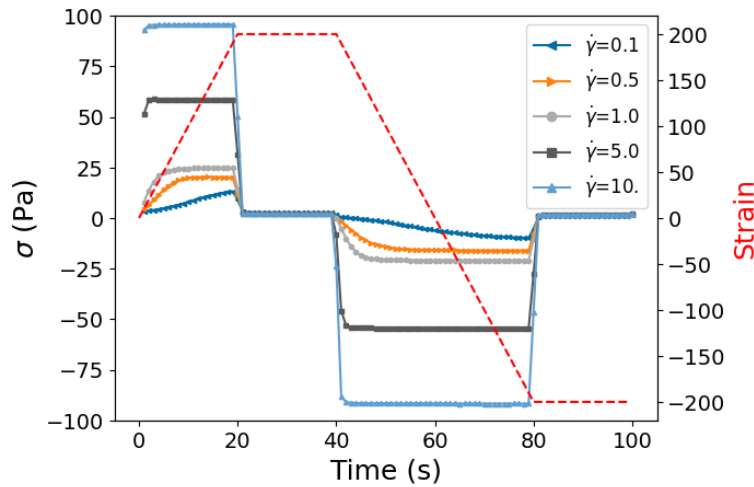


Figure 9: A demonstration of the zero residual elastic stress in SRM 2492 for shear rates ranging from (0.1 to 10) 1/s. The dashed line is the strain for the $\dot{\gamma}_R = 10$ 1/s data, and is indicative of the strain for the other shear rates.

torque values that were averaged to obtain an estimate for that shear rate. Across the entire shear rate range, the torque has reached a constant value upon achieving a total strain of 20.

Because the preshear puts the system into the same state, the shear rate points per decade is not important. For the stability testing, 5 points per decade were used to strike a balance between thoroughness and timeliness.

4.3.3 Preshear Efficacy

This preshear is applied immediately before each measurement. Moreover, the measurement at each shear rate is performed to a constant total strain (20), which means the duration of the measurement depends on the shear rate. However, above a shear rate of 10 1/s, the shear is applied for 3 s to ensure the rheometer has time to reach a steady shear rate.

The effectiveness of removing the effects of shear history on the measurement results is demonstrated in Fig. 11. In the first case, an ascending path, followed by a descending path, is shown with blue filled circles. In the second case, the measurements were taken in “sawtooth” progression, “hopping” among the measurement point ordering (1-7-2-8-3-9...). The points largely lie upon one another. The lowest blue circle, at the lowest shear

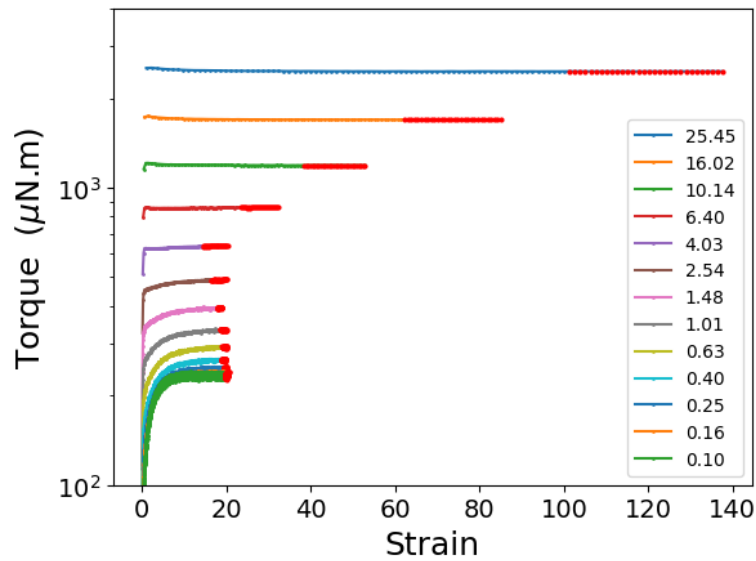


Figure 10: An example of the stress relaxation response when using the preshear method. The values in the legend are the indicated shear rates (in units of 1/s). The values that are averaged to establish an estimate for the torque are the 30 points shown in red.

rate, is most likely a consequence of the sedimentation that can occur over long periods of time.

An advantage of such a preshear is that the measurements can be done in any order, and only once. In the following, the measurements made with the preshear are performed along the ascending path.

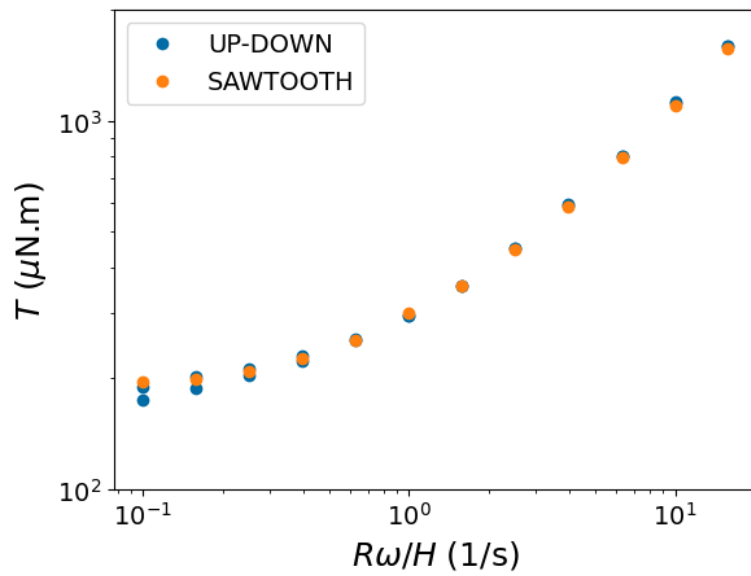


Figure 11: A demonstration of the path independence afforded by the preshear: ascending followed by descending (UP-DOWN); periodically skipping measurement points (SAWTOOTH).

5 Results

The following are the results of the stability testing on two boxes (each) of SRM 2492 and SRM 2493 (paste portion).

All the reported values are from unique samples; there were no replicate measurements from the same specimen jar.

Measurements were performed on a controlled strain rheometer that was calibrated within one year of completing all the measurements.

5.1 Data Analysis

For total clarity, and to support reproducibility, the following is a summary of the data analysis performed on the measurement results.

5.1.1 Viscosity vs. Shear Rate

The viscosity is calculated from the following measurement parameters: the fixture radius R , the indicated gap H° (refer to Eqs. 1 and 5 for determining the corrected gap H), the torque T , and the rotational frequency ω . For rotational parallel plate rheometry, the roughness corrected shear rate is calculated as follows:

$$\dot{\gamma}_R = \frac{R\omega}{H + \epsilon} \quad (10)$$

The shear stress σ is corrected for the non-Newtonian behavior of the liquid [16, 11], giving the following result for the viscosity η as a function of the corrected shear rate $\dot{\gamma}_R$:

$$\eta(\dot{\gamma}_R) = \frac{T}{2\pi\dot{\gamma}_R R^3} \left[3 + \frac{\partial \ln(T)}{\partial \ln(\dot{\gamma}_R)} \right] \quad (11)$$

The partial derivative on the right hand side of Eq. 11 is the non-Newtonian correction to the stress, made by the same arguments as the Weissenberg-Mooney-Rabinowtsch (WMR) correction for capillary flow. For a Newtonian liquid, the quantity in the square brackets is a constant that is equal to 4. For the SRM paste, however, the partial derivative has a sigmoidal shape (on a logarithmic scale), and is shown in Fig. 12 for a C4/L16 specimen. The derivative was calculated numerically, using the `gradient()` function in the Python Numpy package.

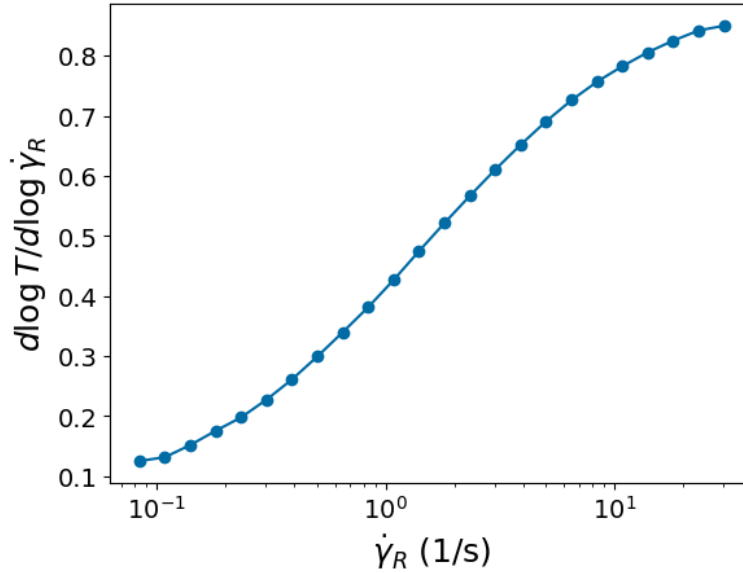


Figure 12: The logarithmic partial derivative of the torque (T) versus the shear rate ($\dot{\gamma}_R$) from Eq. 11 for a C4/L16 specimen.

5.1.2 Expanded Uncertainty in the Mean

The primary contribution to the overall uncertainty is the specimen-to-specimen variability. Each flow curve (viscosity vs. shear rate) shown below represents measurements from a replicate specimen: unique corn syrup solution replicate and unique paste replicate. The estimated value is the average from the replicate specimens. Therefore, the variation among replicate flow curves incorporates the effects of specimen to specimen variability.

The uncertainty in the flow curve values is characterized by the expanded uncertainty in the mean. The sample standard deviation s of the viscosity at each shear rate (from n replicate specimens) is used to calculate the expanded uncertainty in the mean U using the Student-t at confidence $1 - \alpha$ and with ν degrees-of-freedom:

$$U = \frac{s}{\sqrt{n}} t_{1-\alpha/2, \nu} \quad (12)$$

For these calculations, the confidence is expressed as follows: ($1 - \alpha = 0.95$).

5.1.3 Bingham Parameter Estimation

The Certificate values for the Bingham [17] parameters of yield stress and plastic viscosity (within 24 hours of mixing) are shown in Table 6. Measurements made from the paste portion of SRM 2493 should yield the same results.

Table 6: SRM 2492 Certificate Bingham parameter values for yield stress and plastic viscosity, within the first 24 hours; uncertainties represent the expanded uncertainty.

Yield Stress (Pa)	Plastic Viscosity (Pa·s)
25.61 ± 3.47	7.74 ± 1.47

Section 2.3.1 of the SRM 2492 re-certification report [4] provides instruction for collecting data to conduct the Bingham parameter estimation. The process involves 15 ascending shear rates, followed by 20 descending shear rates, spanning the *indicated* (not the corrected) shear rates over the range (0.1 to 50) 1/s. The implication is that this range represents the nominally indicated shear rates, before corrections for fixture plate roughness. Given the reported nominal gap of 0.6 mm and roughness parameter that was on the order of 0.3 mm, and given the Certificate shear rate range extending to 35 1/s, the assumption is that the regression is conducted using uniformly (linearly) spaced shear rates over the range (0.1 to 35.) 1/s.

Although the report indicates that the Bingham parameters can be determined from shear rates that can be equally distributed on either a linear scale or a logarithmic scale, the details of the Bingham parameter estimation for the logarithmically distributed shear rates are not clear. According to the re-certification report [4], the Bingham parameters are estimated from a linear regression of the measured shear stress σ as a function of the corrected shear rate $\dot{\gamma}_R$. The intercept is an estimate for the yield stress σ_y , and the slope is an estimate for the plastic viscosity η_p :

$$\sigma = \sigma_y + \eta_p \dot{\gamma}_R \quad (13)$$

For SRM 2492, however, the shear stress is not a linear function of shear rate over this range; there is negative curvature. As a demonstration, the SRM 2492 Certificate values for viscosity (η) as a function of shear rate ($\dot{\gamma}_R$) (in the first 24 hours) are used to calculate the corresponding shear stress (σ). These values, along with a cubic spline through these data, to guide the eye, are plotted in Fig. 13. In addition, the linear Certificate Bingham equation, using the yield stress and plastic viscosity, is plotted over the same range. For the purposes of performing a regression of the shear stress against the shear rate, the estimation of the Bingham parameters will depend on the individual shear rates chosen for the regression.

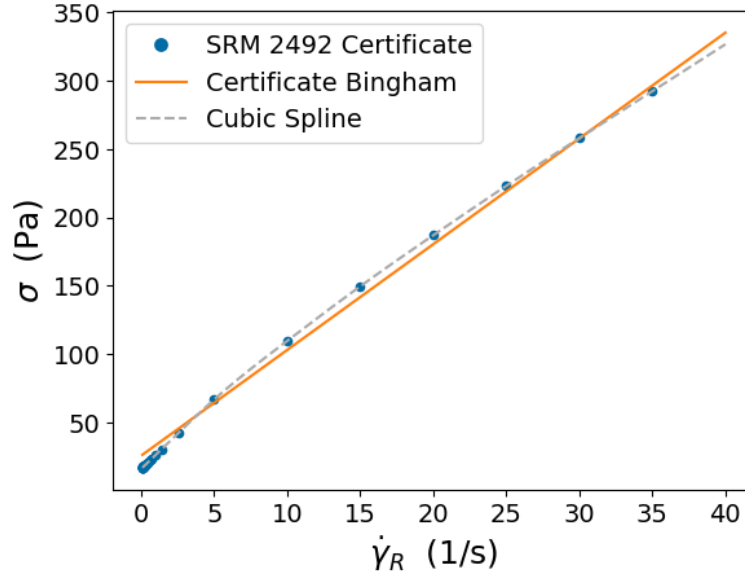


Figure 13: Comparison of the SRM 2492 shear stress (σ), as function of shear rate ($\dot{\gamma}_R$), calculated from the Certificate values (filled circles), a cubic spline through those data (dashed line), and the Certificate Bingham equation (straight line).

This imposes a measurement challenge for SRM 2492. By the time a flow curve measurement (shear stress as a function of shear rate) is completed, one cannot be certain that subsequent measurements on the same sample will be representative. The alternative is to remove the specimen (used to make the flow curve measurement) and load another replicate specimen to make the Bingham parameter estimation, which introduces specimen-to-specimen variation, and increases overall measurement time.

To avoid having to perform the measurement twice (one with linear spacing for Bingham parameters and then another with logarithmic spacing for the flow curve), measurements made using the logarithmic spacing will be used for both. This will be achieved in two steps. First, the data are regressed to the Herschel-Bulkley power law relationship between the shear stress σ and shear rate $\dot{\gamma}_R$:

$$\sigma = \sigma_y^{HB} + k \dot{\gamma}_R^n \quad (14)$$

(The superscript *HB* on the yield stress is to emphasize that the yield stress that was obtained using this equation is different from the yield stress obtained from the Bingham equation.) This relationship is then used to evaluate the stress at shear rates that are equally spaced on a linear scale. More specifically, the lowest shear rate is 0.1 1/s, and the remaining shear rates are evenly distributed between 0.1 1/s and 35 1/s, where these refer to *corrected* shear rates.

This procedure was applied to the Certificate viscosity vs. shear rate data; the shear stress was estimated from the product of the viscosity and the shear rate. As for the Bingham linear regression, the parameters estimate for the Herschel-Bulkley regression depends on the specific shear rates used. For this exercise, the Certificate values are approximated by a cubic spline, which is then evaluated at 20 logarithmically spaced shear rates between 0.1 1/s and 35 1/s. The estimated Herschel-Bulkley parameters are shown in Table 7. The exponent is less than 1, indicating curvature. The direct estimate of yield stress (σ_y^{HB}) is noticeably different from the Certificate value.

Table 7: The Herschel-Bulkley model parameters (see Eq. 14) and standard uncertainties estimated from logarithmically spaced evaluations of a cubic spline through the Certificate values of viscosity vs. shear rate.

σ_y^{HB}	k	n
13.9 ± 0.4	13.2 ± 0.2	0.858 ± 0.005

The Bingham parameters are estimated by evaluating the H-B model at linearly spaced shear rates. The estimated parameters are shown in Table 8, along with the standard uncertainty. The ranges for each parameter overlaps the expanded uncertainty range in the Certificate (see Table 6).

Table 8: The yield stress and plastic viscosity (and standard uncertainties) estimated from linearly spaced shear rates from a regression to the Herschel-Bulkley model using the logarithmically spaced Certificate values.

Yield Stress (Pa)	Plastic Viscosity (Pa·s)
27.8 ± 2.0	7.75 ± 0.10

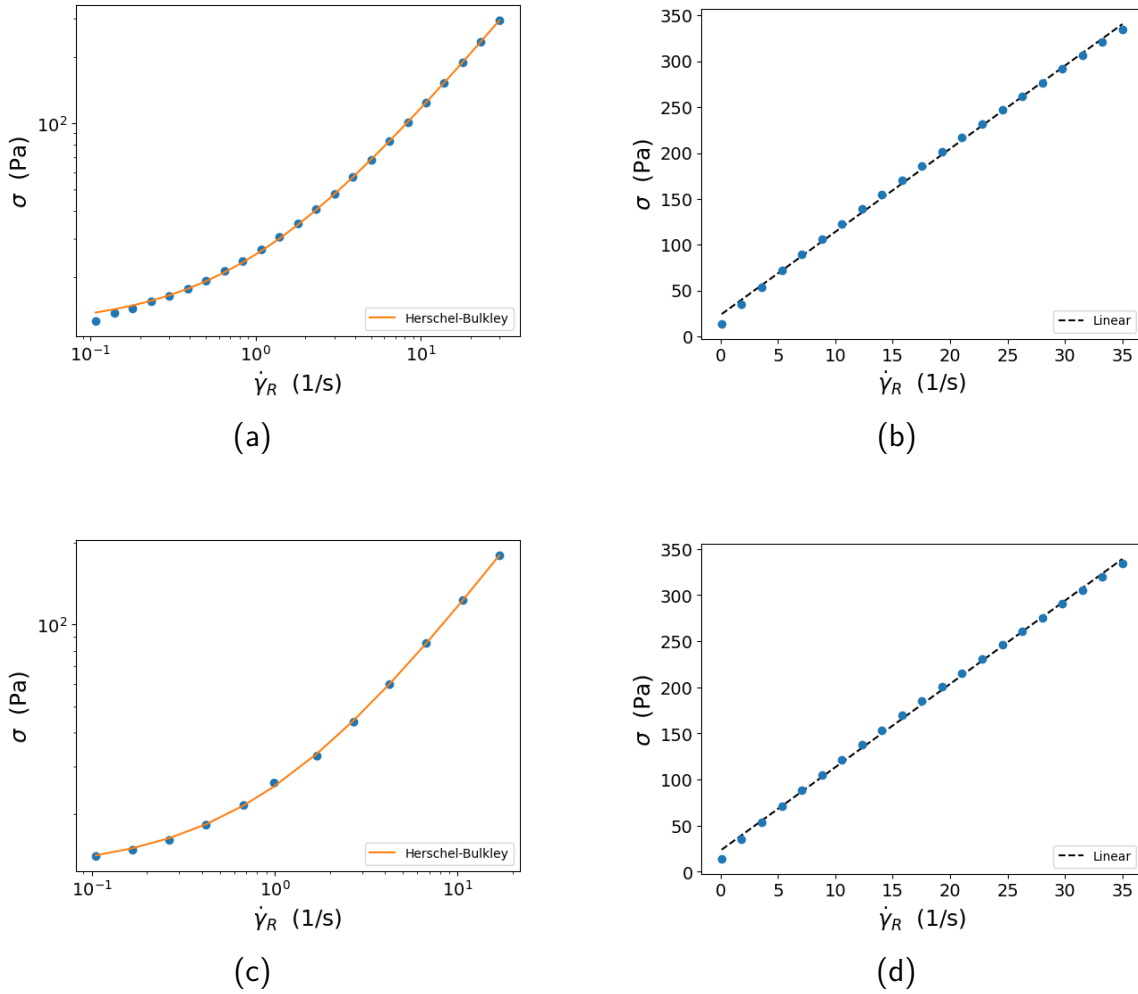


Figure 14: The Herschel-Bulkley and the Bingham regression of shear stress (σ) on shear rate ($\dot{\gamma}_R$) for the same specimen made from C4-L16: (a) and (b) SRM Procedure; (c) and (d) Preshear Procedure.

As a more concrete demonstration of the procedure, the results of the analysis of one C4-L16 specimen is shown in Fig. 14. The figure includes the results for both the SRM measurement procedure and the preshear measurement procedure. Figure 14(a) shows the Herschel-Bulkley regression on the data from the SRM procedure (evaluated at the logarithmically spaced measurement values indicated by filled circles). Figure 14(b) shows the Bingham regression based on linearly spaced shear rates (evaluated from the HB regression, and indicated by the filled circles). Figures 14(c) and (d) demonstrate the corresponding results from the preshear measurement procedure.

5.2 Corn Syrup Solution Viscosity

The corn syrup solution (corn syrup and water) viscosities, for each of the four sample boxes, are shown in Table 9. Each value (in the top four rows) is the average of the five measurements on one distinct replicate specimen. Also shown are the column average \bar{x} and sample standard deviation s_x .

Table 9: Corn syrup solution viscosity for each of the four sample boxes: (Paste) C4-L16 and C5-L19; and (Mortar) C2-L6 and C2-L8. Each value in the top four rows is the average of 5 replicate measurements on the same specimen, but each row represents an independent replicate. Below the top four rows are the column average \bar{x} and sample standard deviation s_x .

	Viscosity (Pa·s)			
	C4-L16	C5-L19	C2-L6	C2-L8
	0.1326	0.1165	0.1403	0.1374
	0.1355	0.1198	0.1423	0.1367
	0.1371	0.1173	0.1362	0.1361
	0.1385	0.1192	0.1363	0.1371
\bar{x} :	0.1359	0.1182	0.1388	0.1368
s_x :	0.0022	0.0013	0.0026	0.0005

There are two striking features of the data in Table 9. The first is that none of the values are within the standard error of the reported viscosity when the SRM was developed: (0.159 ± 0.005) Pa·s. The second is that the viscosity of the solution from box C5-L19 was significantly lower than the other values.

5.3 SRM Procedure Results

The following results are from using the measurement procedure outlined in the SRM reports [3, 4], with further details provided below.

5.3.1 Paste Viscosity

The paste measurements conducted with the SRM Procedure are shown in Figs. 15 and 16 for SRM 2492 (Paste) and SRM 2493 (Mortar), respectively. The figures comprise a plot showing (a) all the individual flow curves (with the mean shown as a dashed line),

and (b) the expanded uncertainty in the mean, compared with the SRM Certificate mean and expanded uncertainties. For the paste SRM and the mortar SRM, there are eight flow curves each.

For both the Paste and the Mortar, the flow curve mean is generally consistent with the SRM Certificate mean values. The differences occur at the extreme shear rate values. More specifically, the two curves seem to intersect.

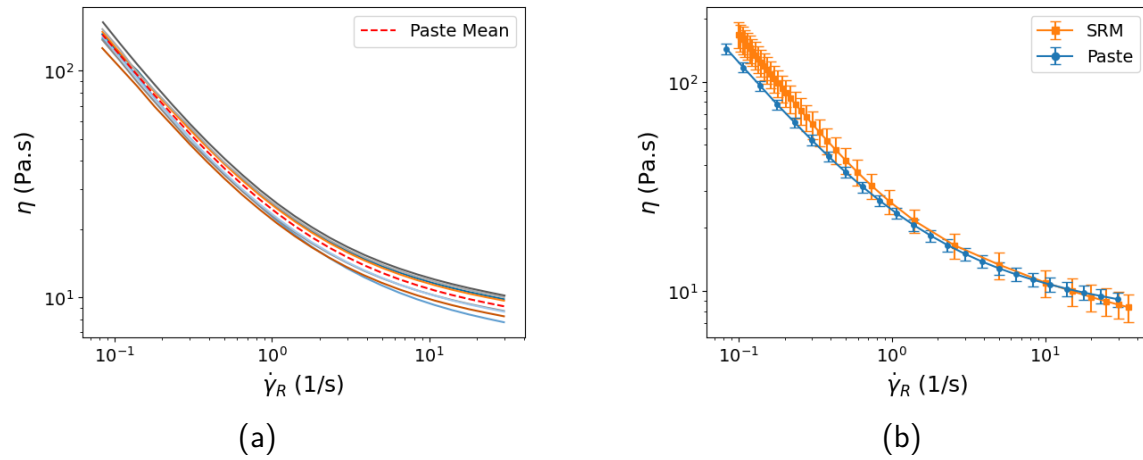


Figure 15: Flow curves for the SRM 2492 (Paste) specimens (C4/L16 & C5/L19) using the SRM Procedure: (a) all the measured data are shown, with the mean value shown as a dashed line; and (b) the expanded uncertainty in the mean, compared with the SRM expanded uncertainty.

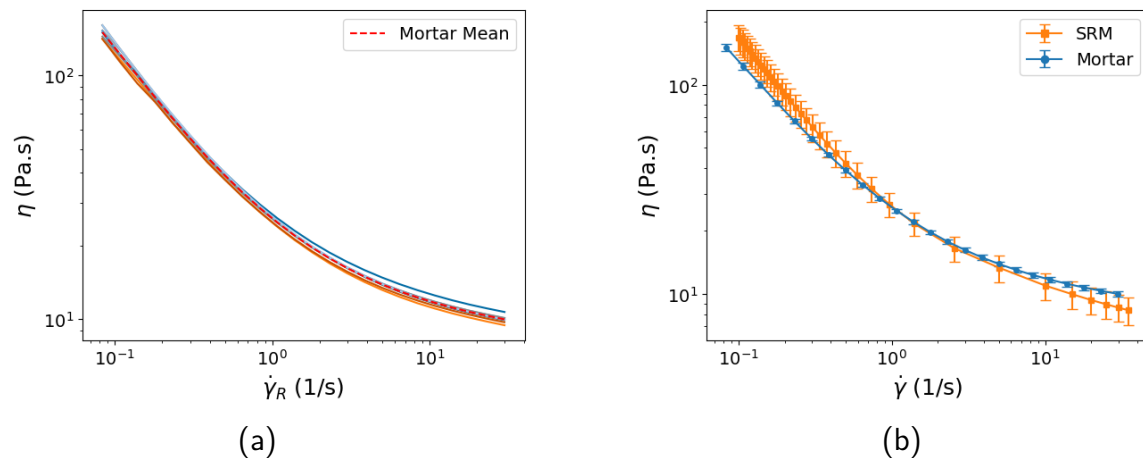


Figure 16: Flow curves for the SRM 2493 (Mortar) paste-component specimens (C2/L6 & C2/L8) using the SRM Procedure: (a) all the measured data are shown, with the mean value shown as a dashed line; and (b) the expanded uncertainty in the mean, compared with the SRM expanded uncertainty.

Although, on average, the paste data were more consistent with the Certificate mean values, the data from the two boxes of SRM 2492 are distinct. In Fig. 17(a), the data from each box is shown in a different color. It is apparent that the data from the two boxes are not representative samples of the same population. The paste viscosity of C5-L19 is lower than that for C4-L16, throughout the range of shear rates. This is consistent with its lower corn syrup solution viscosity shown in Table 9. Moreover, as demonstrated in Fig. 17(b), the C5-L19 expanded uncertainties of the mean do not overlap the expanded uncertainties of the Certificate values throughout the range of shear rates.

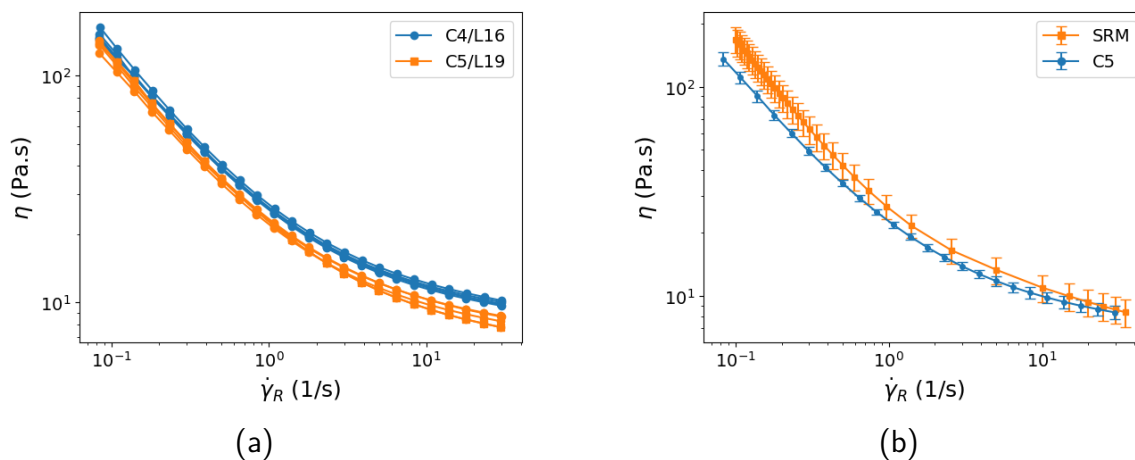


Figure 17: Data from C5/L19: (a) individual data compared with those of C4/L16; and (b) the expanded uncertainty in the mean compared with Certificate values.

5.3.2 Bingham Parameters

The estimated Bingham parameters from each of the SRM Procedure measurements are shown in Table 10. The table includes the sample (column) mean and sample standard deviation.

For samples C4-L16, C2-L6, and C2-L8, the ranges defined by the standard deviation overlap the expanded uncertainty ranges for the Certificate values shown in Table 6. The estimated mean values suggest a systematic change from the Certificate values, consistent with the change in the corn syrup solution viscosity.

Table 10: Bingham plastic viscosity and yield stress using the SRM Procedure. The column mean (\bar{x}) and sample standard deviation (s_x) are shown.

Plastic Viscosity (Pa-s)					Yield Stress (Pa)				
	C4-L16	C5-L19	C2-L6	C2-L8		C4-L16	C5-L19	C2-L6	C2-L8
	9.06	7.09	9.95	9.36		23.50	21.00	24.50	23.40
	8.93	7.61	8.75	9.02		22.90	19.90	22.30	22.40
	9.26	8.05	9.23	9.41		23.50	20.50	23.40	23.00
	9.42	7.96	9.16	9.22		24.50	21.10	23.60	23.70
\bar{x} :	9.17	7.68	9.27	9.25	\bar{x} :	23.60	20.62	23.45	23.12
s_x :	0.19	0.38	0.43	0.15	s_x :	0.57	0.48	0.78	0.49

5.4 Preshear Procedure Results

The following results are from using the preshear procedure outlined above, with further details provided below.

5.4.1 Paste Viscosity

The paste measurements conducted with the Preshear Procedure are shown in Figs. 18 and 19 for SRM 2492 (Paste) and SRM 2493 (Mortar), respectively. The figures comprise a plot showing (a) all the individual flow curves (with the mean shown as a dashed line), and (b) the expanded uncertainty in the mean. The SRM Certificate means and expanded uncertainties are also shown for comparison. For the paste SRM and the mortar SRM, there are eight flow curves.

The distinction between data from C4-L16 and C5-L19 were similar to that for the SRM procedure discussed above. Because the preshear measurement method is not consistent with the prescribed SRM measurement procedure, however, further analysis is delayed to a later section.

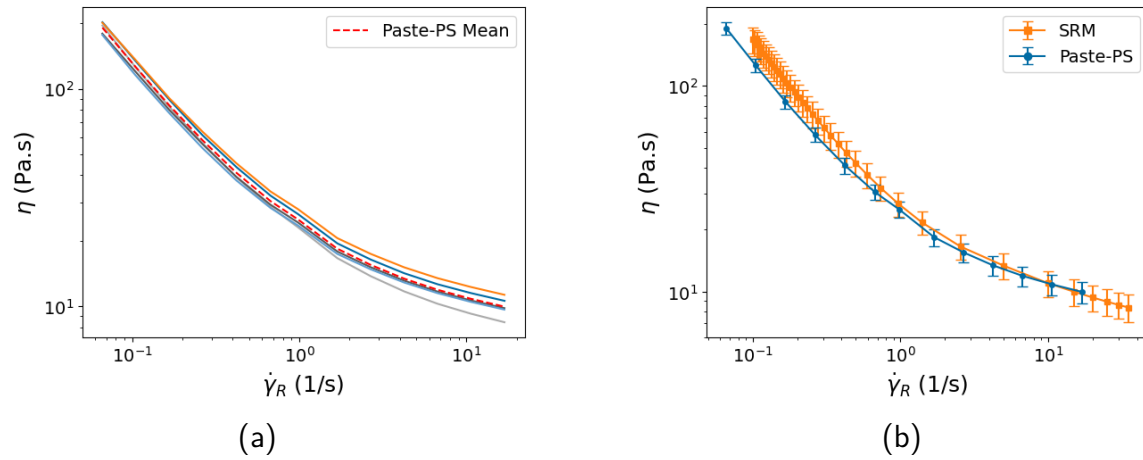


Figure 18: Flow curves for the SRM 2492 (Paste) specimens (C4/L16 & C5/L19) using the Preshear Procedure: (a) all the measured data are shown, with the mean value shown as a dashed line; and (b) the expanded uncertainty in the mean, compared with the SRM expanded uncertainty.

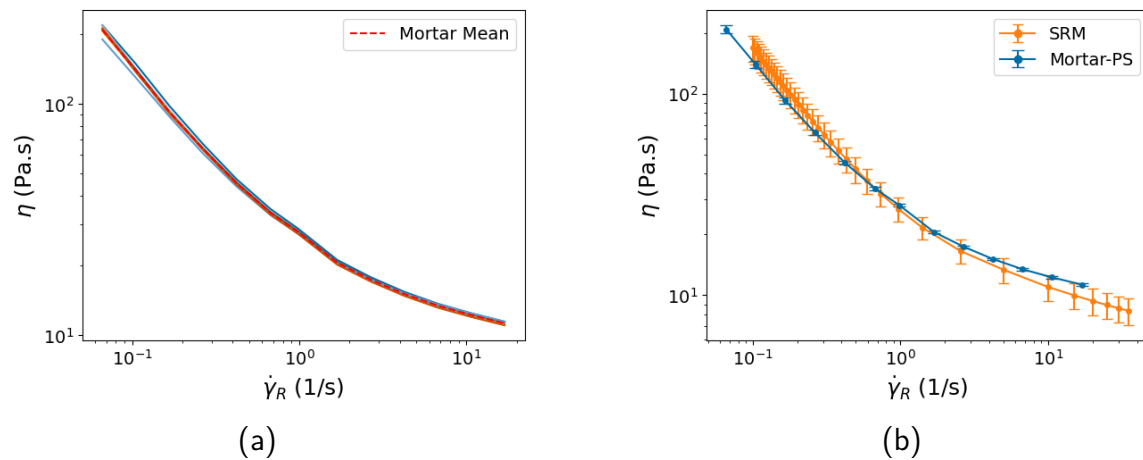


Figure 19: Flow curves for the SRM 2493 (Mortar) paste-component specimens (C2/L6 & C2/L8) using the Preshear Procedure: (a) all the measured data are shown, with the mean value shown as a dashed line; and (b) the expanded uncertainty in the mean, compared with the SRM expanded uncertainty.

5.4.2 Bingham Parameters

The estimated Bingham parameters from each of the Preshear Procedure measurements are shown in Table 11. The table includes the sample (column) mean and sample standard deviation. For the Preshear Procedure, only three measurements were made from each SRM sample.

For samples C4-L16, C2-L6, and C2-L8, the yield stress range defined by the standard deviation overlaps the expanded uncertainty range for the Certificate yield stress shown in Table 6. For the plastic viscosity of the same three samples, the ranges defined by the expanded uncertainty in the means do not overlap the expanded uncertainty range in the Certificate. Because the preshear measurement method is not the required certificate measurement method, this difference is not deemed sufficient to cease sales of the SRM.

Table 11: Bingham plastic viscosity and yield stress using the Preshear Procedure. The column mean (\bar{x}) and sample standard deviation (s_x) are shown.

		Plastic Viscosity (Pa·s)				Yield Stress (Pa)				
		C4-L16	C5-L19	C2-L6	C2-L8	C4-L16	C5-L19	C2-L6	C2-L8	
		9.03	7.06	9.74	9.70	23.10	20.60	25.20	24.40	
		9.60	8.35	9.56	9.80	24.70	21.30	24.50	24.20	
		9.55	8.24	9.40	9.42	24.30	20.70	24.40	24.00	
\bar{x} :		9.39	7.88	9.57	9.64	\bar{x} :	24.03	20.87	24.70	24.20
s_x :		0.26	0.58	0.14	0.16	s_x :	0.68	0.31	0.36	0.16

5.5 Combined Results: C4-L16, C2-L6, and C2-L8

The limestone and corn syrup for SRM 2492 and SRM 2493 are identical, and the pastes are made using the same proportions. Therefore, it is expected that the viscosities would be the same. Given that the C4/L16 viscosity was consistent with the viscosity for C2/L6 and C2/L8, the data are combined into a single data set for comparison purposes. Data from the SRM procedure are shown in Fig. 20. All the flow curves are shown in Fig. 20(a), and the mean and expanded uncertainty in the mean are compared with the corresponding Certificate values in Fig. 20(b). In the former, there is no observable distinction among the data from the three sources, suggesting that they are representative samples from the same population.

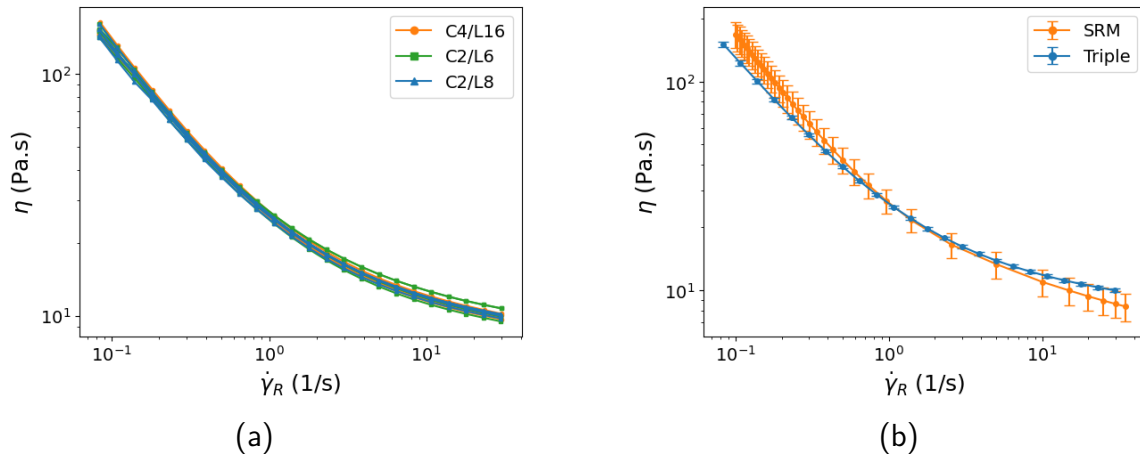


Figure 20: SRM procedure flow curves for the C4/L16, C2/L6, and the C2/L8 boxes: (a) all the data, with the mean value shown as a dashed line; and (b) the expanded uncertainty in the mean (Triple), compared with the SRM expanded uncertainty (SRM).

Similarly, data from the preshear procedure are shown in Fig. 21. All the flow curves are shown in Fig. 21(a), and the mean and expanded uncertainty in the mean are compared with the corresponding Certificate values in Fig. 21(b). As for the data from the SRM procedure, there is no observable distinction among the data from the three sources, suggesting that they are representative samples from the same population.

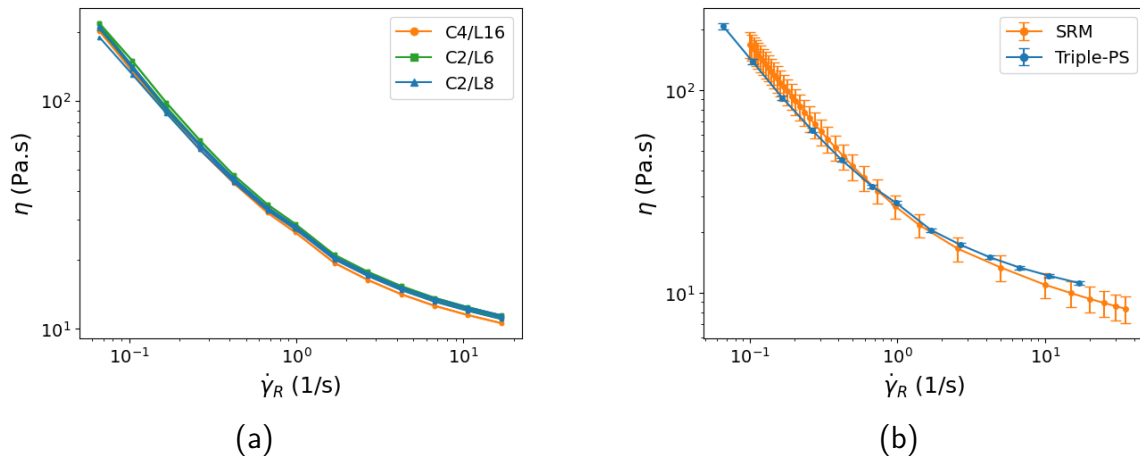


Figure 21: Preshear procedure flow curves for the C4/L16, C2/L6, and the C2/L8 boxes: (a) all the data, with the mean value shown as a dashed line; and (b) the expanded uncertainty in the mean (Triple-PS), compared with the SRM expanded uncertainty (SRM).

A comparison of the two procedures for these three data sets is given in Figure 22. The two procedures result in very similar data. The notable difference is at the lowest shear rates. This is to be expected because the SRM procedure is a constant time measurement, and

the stress growth data used to develop the preshear method indicated that significantly longer measurement times are needed to reach an equilibrium stress at these shear rates.

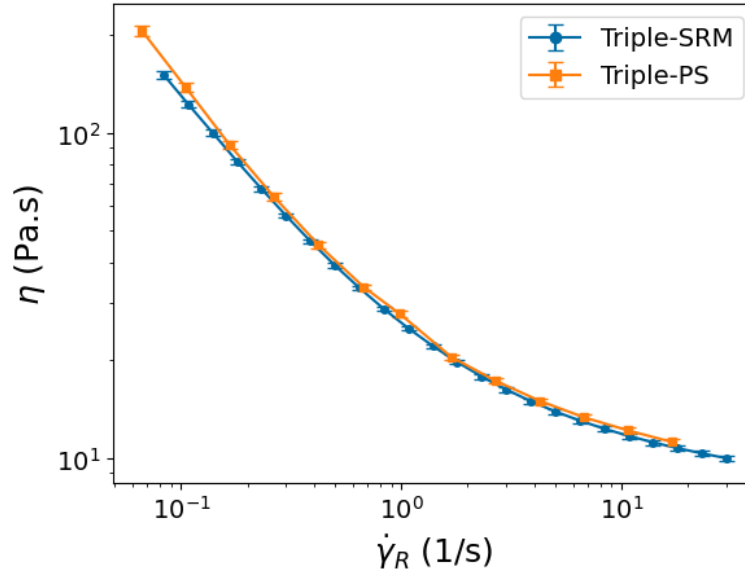


Figure 22: Comparison of SRM Procedure vs. preshear results from samples C4-L16, C2-L6, and C2-L8. Mean and expanded uncertainty in the mean are shown.

Another important difference between these stability data (both the SRM procedure and the preshear procedure) and the Certificate data is the relative expanded uncertainty. The Certificate values for viscosity had a relative expanded uncertainty of approximately 15 % across the entire range of shear rates. The expanded uncertainties in the mean for the SRM procedure are shown in Fig. 23(a), and for the preshear method in Fig. 23(b). The data suggest that the methods used in this Report have reduced the relative expanded uncertainty considerably, compared with the SRM Certificate values.

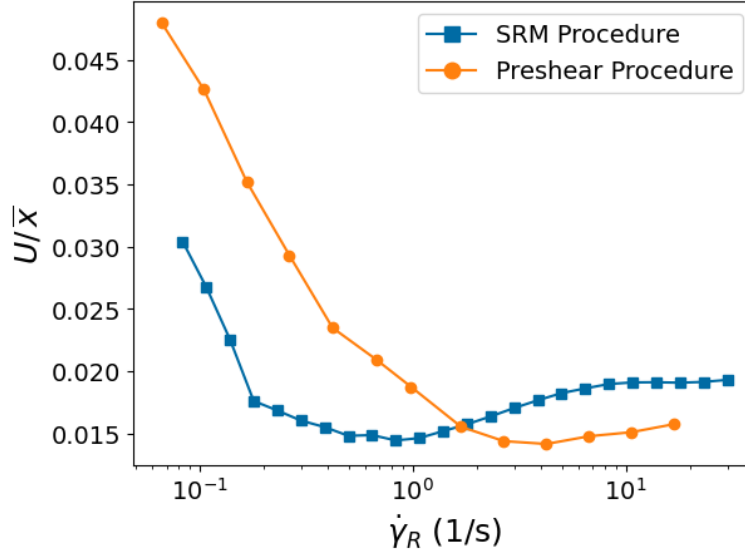


Figure 23: Relative expanded uncertainty in the mean (U/\bar{x}) throughout the shear rate range for the combined data from the three specimens C4/L16, C2/L6, and C2/L8: SRM procedure; and preshear method. For comparison, the SRM Certificate relative expanded uncertainty is approximately 0.15 throughout the shear rate range.

5.6 Viscosity vs. Water Content

Unfortunately, the differences between these results and the Certificate values cannot be explained by changes in the corn syrup water content. Glucose exhibits a Brunauer Type-III (“J”-shaped) water adsorption isotherm, meaning that the water content remains fairly low until exposed to higher relative humidity. Without extended exposure to high humidity, the moisture content should not change dramatically.

Furthermore, adjusting the water content would not change the underlying difference between the results; the two curves cross one another. This conclusion is arrived at by making a comparison between corn syrup and pastes. As explained in the SRM 2493 (Mortar) report [5] and in Martys et al. [18], the effect of the addition of particles to a matrix is to scale the shear rate and the viscosity. If the matrix flow curve can be represented by a function $\eta_{matrix}(\dot{\gamma})$, the flow curve of a paste created by adding particles (η_{paste}) can be written using scaling factors for the shear rate ($\beta_{\dot{\gamma}}$) and viscosity (β_{η}), respectively:

$$\eta_{paste} = \beta_{\eta} \eta_{matrix}(\beta_{\dot{\gamma}} \dot{\gamma}) \quad (15)$$

Given that the matrix viscosity is a monotonically decreasing function of shear rate, and that ($\beta_{\dot{\gamma}} < 1$), and that ($\beta_{\eta} > 1$), the paste viscosity will be greater than the matrix

viscosity at all shear rates. Therefore, adding particles to a matrix can only increase the viscosity. By analogy, adding more corn syrup to water can only increase viscosity (at a given shear rate), not decrease it.

The difference between the measured viscosity flow curve and the Certificate flow curve is not monotonic. The measured flow curve has a viscosity less than the Certificate values at low shear rates, but greater than the Certificate values at high shear rates. Therefore, no amount of changing the corn syrup:water mass ratio will “align” the stability testing results with the Certificate values.

6 Conclusions and Recommendations

Stability testing was conducted for SRM 2492 (Paste) and SRM 2493 (Mortar). The stability testing for SRM 2493 (Mortar) involved only its paste fraction, which is identical to SRM 2492 (Paste) in both composition and proportion. Each SRM is shipped to customers in a box containing the individual components (corn syrup and limestone powder) that the customer uses to formulate the SRM, through the addition of de-ionized water, using precise proportions. Two boxes of SRM 2492 (Paste) and two boxes of SRM 2493 (Mortar) were obtained from the NIST SRM Program. Independent replicate measurements were made from each box.

For each SRM specimen, the viscosity of the corn syrup and water mixture was measured before adding the limestone powder. The purpose of this measurement was to gauge consistency of the mixing procedure, and to compare values among the different SRM specimens. The mixture viscosity for three of the specimens (one of the SRM 2492 and both of the SRM 2493) were within approximately 2 % of one another. The mixture viscosity of the last SRM 2492 specimen differed from the others by nearly 14 %.

This difference among the corn syrup and water mixture viscosities was borne out in the measurement results after the limestone was added. For the three specimens having similar corn syrup and water viscosity values, the paste viscosity values were within a few percent of one another and within the Certificate expanded uncertainty, across the entire shear rate range. For the specimen with the changed value in the corn syrup and water viscosity, the paste viscosity was not within the Certificate expanded uncertainty for a considerable range of shear rate values.

6.1 SRM 2492 (Paste)

The measurements indicate that the corn syrup in some of the SRM 2492 (Paste) boxes could have changed significantly. The result of the change is measurement results that would not be within the expanded uncertainty of the Certificate value. Because of this, and out of an abundance of caution, it has been decided to discontinue sales of SRM 2492 (Paste).

Anticipating any changes in the corn syrup may be very difficult. The results from the unchanged SRM 2492 (Paste) were indistinguishable from both of the SRM 2493 (Mortar) specimens. Therefore, the changes in the corn syrup are not gradual, over a long time period. If they were, periodic sampling could be used to predict the expected lifetime of a particular SRM. Instead, the only way to know if the corn syrup that is in a particular box

of SRM has not changed is to measure the viscosity of the resulting corn syrup and water mixture, which would have to be performed for each box of SRM. This is not a practical solution.

6.2 SRM 2493 (Mortar)

Measurements on the SRM 2493 specimens indicated the materials will still yield results within the expanded uncertainty of the Certificate values. Given that changes were observed for SRM 2492 (Paste), which was stocked 3 years prior to SRM 2493, the next stability testing for SRM 2493 (Mortar) should be no more than 3 years hence (2028).

It should be noted, however, that an absence of an observed change in SRM 2493 is not conclusive. Conversely, there is no evidence to warrant stopping sales. Admittedly, this was a small sample size - only two boxes of SRM 2493 were tested. Therefore, it is recommended that SRM 2493 (Mortar) customers measure the viscosity of the corn syrup and water mixture to ensure that the corn syrup has not changed.

6.3 SRM 2492 Substitution

Until a replacement for SRM 2492 can be established, the need for a paste rheology SRM can still be met. An alternative to SRM 2492 (Paste) is to use the paste portion of SRM 2493 (Mortar) as a direct substitute. The paste portion of SRM 2493 is identical to SRM 2492 in both composition and proportions. The drawback (to the customer) is that SRM 2493 (Mortar) is more expensive than SRM 2492 (Paste).

6.4 Reduced Measurement Uncertainty

The process of conducting the stability testing has resulted in refinements to the preparation and measurement procedures that reduced the expanded uncertainty in the result. The reduction was at least a factor of 3 throughout the Certificate shear rate range, and at least a factor of 7 for shear rates greater than 1 s^{-1} .

The preparation improvements focused on sample mixing and fixture setup. Thorough, consistent mixing was achieved using a centrifugal planetary mixer, which ensured mixing throughout the entire specimen, with a minimum of incorporated air, and allowed for smaller specimens. The refinements to the fixture surface preparation and setting the

gap helped to achieve consistent results. These small changes in procedure are important because the relative uncertainty associated with each of these steps combine to set a lower bound on the relative uncertainty in the final result.

6.5 Paste SRM Next Steps

In the future, a decision must be made whether to develop a replicate of SRM 2492 with new corn syrup, or to develop one or more new SRMs having viscoelastic properties that are applicable to a range of concrete construction methods.

A possible alternative mechanism for moving forward would be to develop a NIST Research Grade Test Material (RGTM), which are materials used during the prototyping and development phases of reference material development.² This makes them ideal for developing consistent industry-wide measurement practice, and for collaborating on the development of a new SRM. These materials need to be homogeneous and stable, but the properties have not been quantitatively evaluated to the degree of an SRM.

One candidate for a paste RGTM would be a mixture of quartz powder in glycerol. The quartz particle size distribution and its total volume fraction could be varied to achieve a range of viscoelastic properties, spanning from self-consolidating concrete to additive construction materials. The glycerol has a viscosity that is greater than the corn syrup and water mixture, but is chemically stable and has a lower volatility than the corn syrup solution.

These two materials may be ideal for achieving consistency and stability. The RGTM could comprise two or three quartz powders, each with a different particle size distribution. To create a reference material, the collaborator would purchase glycerol (of a specified minimum purity). A reference value would be associated with a specific formulation of one or more of the powders and the glycerol. The quartz powder would be stable, and the glycerol would be purchased just prior to measurement, thus ensuring stability.

²<https://www.nist.gov/srm/srm-definitions>

References

- [1] Ferraris C, Brower L, et al. (2001) Comparison of concrete rheometers: International tests at Ipcp (nantes, france) in october 2000 (National Institute of Standards and Technology, U.S. Department of Commerce, Washington, D.C.), Available at https://tsapps.nist.gov/publication/get_pdf.cfm?pub_id=860574.
- [2] Brower L, Ferraris C (2003) Comparison of concrete rheometers. *Concrete International* 25:41–47.
- [3] Ferraris C, Stutzman P, Guthrie W, Winpigler J (2012) Certification of SRM 2492: Bingham Paste Mixture for Rheological Measurements (National Institute of Standards and Technology, U.S. Department of Commerce, Washington, D.C.), Available at https://shop.nist.gov/ccrz__ProductDetails?sku=2492&cclcl=en_US.
- [4] Olivas A, Ferraris C, Guthrie W, Toman B (2015) Re-certification of SRM 2492: Bingham Paste Mixture for Rheological Measurements (National Institute of Standards and Technology, U.S. Department of Commerce, Washington, D.C.), <https://doi.org/10.6028/NIST.SP.260-182>
- [5] Olivas A, Ferraris C, Martys N, George W, Garboczi E, Toman B (2017) Certification of SRM 2493: Standard Reference Mortar for Rheological Measurements (National Institute of Standards and Technology, U.S. Department of Commerce, Washington, D.C.), <https://doi.org/10.6028/NIST.SP.260-187>. Available at https://shop.nist.gov/ccrz__ProductDetails?sku=2493&cclcl=en_US
- [6] Ferraris C, Martys N, Peltz M, George W, Garboczi E, Toman B (2019) Certification of SRM 2497: Standard Reference Concrete for Rheological Measurements (National Institute of Standards and Technology, U.S. Department of Commerce, Washington, D.C.), <https://doi.org/10.6028/NIST.SP.260-197>. Available at https://shop.nist.gov/ccrz__ProductDetails?sku=2497&cclcl=en_US
- [7] National Institute of Standards and Technology (2022) SRM 2492 Certificate, <https://tsapps.nist.gov/srmext/certificates/2492.pdf>.
- [8] Tschoegl N (1989) *The Phenomenological Theory of Linear Viscoelastic Behavior: An Introduction* (Springer-Verlag). <https://doi.org/10.1007/978-3-642-73602-5>
- [9] Divoux T, Grenard V, Manneville S (2013) Rheological hysteresis in soft glassy materials. *Physical Review Letters* 110:018304.

- [10] Ferraris C, Geiker M, Martys N, Muzzatti N (2007) Parallel-plate rheometer calibration using oil and computer simulation. *Journal of Advanced Concrete Technology* 5(3):363–371.
- [11] Connelly R, Greener J (1985) High-shear viscometry with a rotational parallel-disk device. *Journal of Rheology* 29(2):209–226.
- [12] Pipe C, Majmudar T, McKinley G (2008) High shear rate viscometry. *Rheol Acta* 47:621–642.
- [13] Kramer J, Uhl J, Prud'homme R (1987) Measurement of the viscosity of guar gum solutions to $50,000 \text{ s}^{-1}$ using a parallel plate rheometer. *Polym Eng Sci* 27(8):598–602.
- [14] Choi J, Rogers S (2020) Optimal conditions for pre-shearing thixotropic or aging soft materials. *Rheologica Acta* 59:921–934.
- [15] Donley G, Martys N, Del Gado E, Snyder K (2026) Path-independent flow characterization of model yielding pastes. *Rheologica Acta* 65:1–12. <https://doi.org/10.1007/s00397-026-01553-y>
- [16] Bird R, Armstrong R, Hassager O (1977) *Dynamics of Polymeric Liquids: Volume 1. Fluid Mechanics* (John Wiley & Sons).
- [17] Bingham E (1916) An investigation of the laws of plastic flow. *Bulletin of the Bureau of Standards* 13:309–353.
- [18] Martys N, George W, Chun BW, Lootens D (2010) A smoothed particle hydrodynamics-based fluid model with a spatially dependent viscosity: application to flow of a suspension with a non-newtonian fluid matrix. *Rheologica Acta* 49(10):1059–1069.